Doctoral Dissertation

ADSORPTION OF PHOSPHATE BY CALCINED MG_3-FE LAYERED DOUBLE HYDROXIDE

焼成した Mg_3–Fe 型層状複水酸化物を用いたリン酸イオンの吸着

XIAOFENG SUN

Division of Environmental Science and Engineering

Graduate School of Science and Engineering

Yamaguchi University, Japan

2014.3

博士論文

Doctoral Dissertation

焼成した Mg_3–Fe 型層状複水酸化物を用いたリン酸イオンの吸着

ADSORPTION OF PHOSPHATE BY CALCINED MG_3-FE LAYERED DOUBLE HYDROXIDE

孫肖潩

SUN XIAOFENG

A dissertation submitted to the Division of Environmental Science and Engineering of Yamaguchi University in partial fulfillment of the requirements for the degree of Doctor of Engineering

Advisor: Prof. Tsuyoshi Imai
(Div. of Environmental Science and Engineering, Fac. of Engineering)

Committee Members:
Prof. T. Imai (Div. of Environmental Science and Engineering)
Prof. M. Sekine (Div. of Civil and Environmental Engineering)
Prof. M. Niinae (Div. of Environmental Science and Engineering)
Assoc. Prof. K. Yamamoto (Div. of Civil and Environmental Engineering)
Assoc. Prof. T. Saeki (Div. of Environmental Science and Engineering)

山口大学大学院理工学研究科環境共生系専攻
Division of Environmental Science and Engineering
Graduate School of Science and Engineering
Yamaguchi University, Japan

2014.2

ACKOWLEGEMENT

I am indebted to a lot of people to success this dissertation and would like to spend this space to express my gratefulness to my academic advisors, family and friends for invaluable support.

I am respectful and appreciative to my academic advisor, Prof. T. IMAI who has provided finical support, expert suggestion, and warm encouragement during my stay in Japan.

My sincere gratitude is also expressed to Pro. Z. J. Zhang (Shanghai Jiao Tong University, China) who suggested me to study in Yamaguchi University, and gave me many guides during my study here.

I am also indebted to Prof. M. SEKINE, Prof. NIINAE, Assoc. Prof. K. YAMAMOTO and Assoc. Prof. T. SAEKI for serving as members of the committee.

Thank also extend to Prof. M. UKITA, Assoc. Prof. T. HIGUCHI, Asst. K. ARIYO, who gave many advises to improve my research.

My deepest gratitude to T. YAMAMOTO, S. NAKAZONO, K. AKAGI, J. WEI, X.H. CHENG, H. RAFIANI, J. TEEKA, A. NOVI, L.V. TUAN, S. GATOTO, V. T. HUY, K. EVI, P. KANTHIMA, A. AIFAI, F. RINA, H. RIYANTO and other friends in Japan for their kind help and assistance.

Finally, I would like to express my heartfelt gratitude to my family in both Japan and China who gave support always during my life time.

ABSTRACT

Phosphorus is an essential nutrient among plants and animals, but it is a non-renewable resource, and the global commercial phosphate reserves will be depleted in 50–100 years. While global phosphorus scarcity is likely to be one of the severest problems of the 21st century. Therefore, there are concerns about ensuring long-term and stable availability of phosphorus resources from recovery processes in the future. So far, there are a number of technologies (chemical precipitation, biological phosphorus removal, crystallization, adsorption, etc.) which can be used to removal, and recovery of phosphorus from phosphorus contained aqueous solution within a sustainable strategy. In order to remove and recover phosphate resource from aqueous solutions by adsorption method, we synthesized a novel adsorbent of calcined Mg_3-Fe layered double hydroxide (LDH), and examined the phosphate adsorption performance in synthesized NaH_2PO4 solutions. Furthermore, we applied this adsorbent to actual anaerobic sludge filtrate to investigate its practical adsorption capacity and reusability.

In chapter 1, the general, objectives and structure of my studies were described.

In chapter 2, the significance of phosphorus resources and its global scarcity, the alternative phosphorus removal technologies were introduced, following with the history of layered double hydroxides which included the structure, synthesis, characterization, their potential use for removing inorganic contaminants such as oxyanions and monoatomic anions from aqueous solutions by the process of adsorption and adsorption mechanism.

In chapter 3, a series of Mg-Fe LDHs after calcination were synthesized by using co-precipitation method under low super-saturation conditions. Several factors such as Mg/Fe molar ratio, pH, coexisting anions, adsorption kinetics, adsorption isotherm and desorption efficiency that affect the phosphate adsorption capacity were discussed via batch experiments. It was found that the highest phosphate adsorption capacity was obtained with Mg/Fe ratio of 3 and calcined at 573 K, which was in agreement with the results of the powder X-ray diffraction (XRD). The appropriate pH value was found to be 6.9. The distribution coefficient (K_d) revealed good adsorption selectivity of calcined Mg_3-Fe LDH for phosphate in a mixed solution with NaCl, $NaNO_3$, and Na_2SO_4. The adsorption kinetics, which was studied using a pseudo-second-order model, showed high adsorption capacities of 77.5 mg-P/g in NaH_2PO_4 solution. The adsorption isotherms showed that the phosphate uptake process was better fit with the Freundlich model than with the Langmuir model. The adsorbed phosphate can be effectively desorbed (73%) by the addition of a 0.1 M NaOH solution.

As a continuation of batch experiments in previous chapter, we focused on evaluating the performance of granular calcined Mg_3-Fe LDHs for removing phosphate ions in a fixed-bed column using synthesized NaH_2PO_4 solutions in chapter 4. The effects of parameters such as bed-height, flow rate, and initial concentration on a breakthrough curve were investigated. Widely used column adsorption models were applied to validate the experimental data. Furthermore, the adsorption mechanism was proposed according to results of model fitting. We also assessed the performance of the granule-packed fixed-bed column in removing and recovering phosphate from

actual anaerobic sludge filtrate. Finally, exhaustion-regeneration cycles were employed to investigate the reusability of the adsorbent. It was found that an increase in bed height and initial phosphate concentration or a decrease of flow rate improves the adsorption capacity. The Bed Depth Service Time (BDST) model was found to satisfactorily predict the breakthrough curve up to 60% breakthrough at a 0.024 L/h flow rate and 10 mg/L initial phosphate concentration. The Clark model was found to be the most suitable for fitting experimental data with respect to various bed heights, flow rates, and initial phosphate concentration values, followed by the Thomas and Yoon-Nelson models (in decreasing order of suitability). We found the applicability of this adsorbent to phosphate recovery from anaerobic sludge filtrate because of its good selectivity in a system of coexisting anions, high adsorption capacity, and acceptable reusability.

Chapter 5 makes conclusion and future work of this study. As far as we are aware, this calcined Mg_3-Fe LDH adsorbent has potential for the application of phosphate adsorption from aqueous solution. In addition, several important considerations should be taken in the design of LDH adsorption system. 1) The supernatant from the anaerobic sludge filtrate contains medium suspended solids, which could foul the ion exchanger and cause potential clogging problems. Therefore, an economical pretreatment such as dual-media or multi-media filters would be required for a pilot application. 2) The further processing of recovered phosphate from phosphate-desorbed alkaline solution to useful finalized products such as calcium phosphate, hydroxyapatite, or magnesium ammonium phosphate need to be investigated, and the proper disposal of the restored desorption solution also needs to be addressed.

学位論文要旨

リンはすべての植物と動物にとって必須な栄養素であるが、リンは枯渇性資源であり、世界のリンの可採掘な埋蔵量が 50ー100 年で枯渇するといわれている。それゆえに全世界的なリン資源の不足は、21 世紀の最も厳しい資源問題の一つとなる可能性が高まっている。したがって、近い将来的に排水処理過程からのリン資源の長期的かつ安定的な回収プロセスの確立が必須である。現在までに、リンを含有する排水等からリンを除去・回収するために多数の技術（化学的沈殿法、生物学的リン除去法、結晶法、吸着法等）が開発されている。この中でも本研究では吸着法によるリンの回収法に着目した。すなわち、水溶液中に存在するリン酸イオンを高効率に除去・回収するために、新規に吸着剤として Mg-Fe 型層状復水酸化物（LDH）を種々の条件を変えて焼成し、これらを用いて NaH_2PO_4 溶液からのリン酸吸着性能を調べ、その最適合成条件について検討した。さらに、その実際の吸着能力及び再利用性を把握するために、実下水処理施設の嫌気性消化槽からのろ液に、この吸着剤を適用しその能力を確認し、本研究で焼成した LDH の有用性を検討した。

第 1 章では、本研究の目的および論文の構成について説明した。

第 2 章では、リン資源の重要性とその世界的な枯渇の危機的状況、さらにリンの除去・回収に関する技術開発の現状について述べた。続いて、層状復水酸化物の構造、その合成と特性評価及びそれによる水溶液からのオキシアニオンや単原子アニオン等の吸着による無機汚染物質の除去可能性と吸着メカニズム等、層状復水酸化物の歴史についても述べた。

第 3 章では、低過飽和条件下で共沈殿法を用い、Mg-Fe の比率に条件を変化させて、種々の Mg-Fe 型 LDH を焼成した。焼成した Mg-Fe 型 LDH について、pH 値、共存する陰イオン、吸着速度、吸着等温線および脱着効率等のリン酸吸着能力に影響を与える要因について、回分（バッチ）実験により検討した。その結果から、最もリン酸の吸着能力が高かったのは「Mg/Fe の比率が 3 の場合で 573 K の焼成温度」であることが明らかとなった。また、これは X 線回折（XRD）による解析結果とも一致した。次に吸着最適 pH 値が 6.9 であることも明らかとなった。分配係数（K_d）の解析から、本研究で焼成した Mg_3–Fe 型 LDH は NaCl、$NaNO_3$、Na_2SO_4 の混合溶液中で良好なリン酸の吸着選択性があることが明らかとなった。擬似二次モデルを用いて検討した吸着動力学解析から、本研究で焼成した Mg_3–Fe 型 LDH は NaH_2PO_4 溶液中で 77.5 mg-P/g の高い吸着能力を示した。さらに、吸着等温線に関する解析から、リン酸の吸着プロセスはラングミュアモデルに比べフロイントリッヒモデルとより高い相関性（適合性）を示した。加えてリン酸吸着後の Mg_3–Fe 型 LDH に 0.1 M NaOH 溶液を添加することによって、吸着されたリン酸を効果的に脱離（73%）させることができた。

第 4 章では、前章のバッチ実験から引き続き、固定床カラムを用いた連続実験により、焼成した Mg_3-Fe 型 LDH による NaH_2PO_4 溶液からのリン酸イオンの除去性能を評価した。すなわち、カラム高さ、流速、および初期濃度等のパラメータの影響を検討した。この際に現在一般に広く用いられている既存のカラム吸着モデルを実験データを検証するために適用し、フィッティング解析を行った。さらに、その解析結果から、吸着メカニズムについて検討した。また、

固定床カラムを用いて焼成した Mg_3-Fe 型 LDH による実際の排水処理施設における嫌気性汚泥ろ液からリン酸塩を除去し、回収する実験を行った。最後に、吸着ー脱離サイクルに関する繰り返し実験を行い、吸着剤の再利用性を検討した。実験結果から、カラム高さの増加及びリン酸塩の初期濃度あるいはその流量の減少が、吸着容量を向上させることが見出された。BDST モデルは、0.024 L / h の流速及び 10mg / L の初期リン酸塩濃度の条件下において 60 %漏出までの破過曲線を良好に予測できた。クラークモデルは、様々なカラム高さ、流速、および初期リン濃度値に対して実験データを最もよく再現できた。続いて、トーマスモデル、ユン· ネルソンモデルの順であった。嫌気性消化ろ液からのリン吸着実験の結果から、本吸着剤（焼成した Mg_3-Fe 型 LDH）が共存する陰イオンの共存化で優れたリン酸の選択性、高い吸着容量、および許容可能な再利用性を有することが示された。

第 5 章では、本研究の結論と今後の課題について述べた。本研究で開発した Mg_3-Fe 型層状復水酸化物（LDH）リン酸吸着剤のリン除去・回収性能の有効性が明らかとなったと考えられる。なお、LDH 吸着システムの設計に際し以下の点を考慮する必要がある。1）嫌気性消化ろ液には通常イオン交換能を低下させ、カラム内の目詰まりの問題を引き起こす可能性の高い浮遊物質（SS）が含まれている。したがって、スケールアップ時には複数のカラムを組み合わせたデュアルメディアあるいはマルチメディア· フィルタ等の前処理が必要であろう。2）また、アルカリ溶液を用いて吸着されたリン酸を脱離し、その回収されたリン酸からリン酸カルシウム、ヒドロキシアパタイト（HAP）、あるいはリン酸マグネシウムアンモニウム（MAP）等の再利用の容易な有用生成物へと変換するために、さらなる効率的プロセスを開発する必要があり、再利用を含めた脱着溶液の適切な処分にも対処する必要がある。

Contents

List of figures

List of tables

CHAPTER 1

INTRODUCTION

1.1 General

Recently, due to the global phosphorus resource scarcity, there are concerns about ensuring long-term and stable availability of phosphorus resources from recovery processes. Especially, the phosphorus removal from waste streams has been extensively studied which can potentially be used within a sustainability strategy. The widely applied methods include chemical precipitation, biological phosphorus removal, crystallisation and adsorption. Among them, adsorption of phosphorus from wastewater is a cost-effective and environment-friendly technology, by which the chemical sludge production is small and the adsorbed phosphorus can be easily recovered.

Layered double hydroxides (LDHs) has been paid considerable attention for their application in removing negatively charged species through both surface adsorption and anion exchange.

In our research, we synthesized a novel calcined Mg_3-Fe LDH adsorbent and investigated its phosphate adsorption performance via both batch and continuous experiments. Finally, we applied actual anaerobic sludge filtrate, which contained high concentration of phosphate as a species of wastewater steam to evaluate the feasibility of the adsorbent.

1.2 Objectives

The aim of this research is to:

1. Develop a novel Mg-Fe LDH type adsorbent with high phosphate adsorption

capacity.

2. Investigate the effects of the Mg/Fe molar ratio, influence of competitive anions, adsorption kinetics, phosphate adsorption isotherm, phosphate desorption under batch tests in order to understand its mechanisms of adsorption dynamic kinetics and adsorption isotherm.
3. Investigate the effects of parameters such as bed-height, flow rate, and initial concentration on a breakthrough curve under continuous fixed-bed column tests and applied the widely used column adsorption models to validate the experimental data.
4. Apply Mg-Fe LDH type adsorbent to actual anaerobic sludge filtrate to investigate its practical adsorption capacity and reusability.

1.3 Structure of this study

Chapter 2 presents a literature reviews on the significance of phosphorus resources, the alternative phosphorus removal technologies, and the history of layered double hydroxides.

Chapter 3 and Chapter 4 are the core parts of this thesis.

In Chapter 3, we describe the synthesizing process of calcined Mg_3-Fe LDH adsorbent, the flow chart of batch experiments, and investigate several factors which affect the phosphate adsorption process. Meanwhile, the mechanisms of adsorption dynamic kinetics and adsorption isotherm are also discussed according to above-mentioned results.

Chapter 4 concentrates on the performances of phosphate adsorption process on continuous tests by using a fix-bed column. The effects of parameters such as bed-height, flow rate, and initial concentration on a breakthrough curve are investigated, and several applied the widely used column adsorption models to validate the experimental data.

In the following parts of Chapter 4, i attempt to apply the calcined Mg_3-Fe LDH adsorbent to actual anaerobic sludge filtrate to investigate its practical adsorption

capacity and reusability.

Chapter 5 makes short conclusions for this study.

CHAPTER 2

LITERATURE REVIEW

2.1 Significance of phosphorus resource

The element phosphorus is essential to all life (e.g. plants, animals and bacteria) and is a key ingredient in fertilizers to sustain high crop yields. Phosphorus has no substitute in food production and in a world of 9 billion people by 2050, securing sufficient phosphorus will be critical for future food security. Yet the world's main source of phosphorus, phosphate rock, is non-renewable and becoming increasingly scarce and expensive. Peak phosphorus was estimated to occur by 2035, after which demand would outstrip supply (Cordell et al, 2009). While the exact timeline might be uncertain, there are no alternative sources of phosphorus on the market that could replace the current global production of 20 million tonnes (Mt) of P from phosphate rock. Recent scientific and popular science articles have explicitly drawn attention to the challenges of global phosphorus scarcity (Déry and Anderson, 2007, Rosemarin et al, 2009, Vaccari, 2009, Smit et al, 2009), however there is still a lack of policy debate and action.

While global phosphorus scarcity is likely to be one of the greatest challenges of the 21st century, it is possible to avert a crisis with concerted action. One reason behind such optimism is that the current food production and consumption system is highly inefficient with respect to phosphorus use. Indeed, while approximately 19 Mt a^{-1} of P is mined from phosphate rock specifically for food production (Heffer and Prud'homme, 2009), only a fifth of this phosphorus actually reaches the food consumed by the global population (Cordell et al, 2009). Phosphorus is lost – permanently or temporarily – at all key stages of the food system, from mine to field to fork, meaning there are substantial opportunities for improving efficient use and reuse.

Global phosphorus security is directly linked to food security, environmental

protection and farmer livelihoods and can be defined as ensuring that "all the world's farmers have access to sufficient phosphorus in the short and long term to grow enough food to feed a growing world population, while ensuring farmer livelihoods and minimising detrimental environmental and social impacts". However there is no single solution to achieving a sustainable phosphorus cycle. A recent global phosphorus scenario analysis (Fig. 2-1) indicated that meeting the increasing long-term phosphorus demand would likely require demand management measures to reduce business-as-usual demand by two-thirds, and the remaining third could be met through a high recovery rate of phosphorus from human excreta, manure, food waste and mining waste. However achieving such a high recovery and reuse scenario will undoubtedly require substantial changes to physical infrastructure, new partnerships and strategic policies to guide phosphorus recovery and reuse in an integrated way.

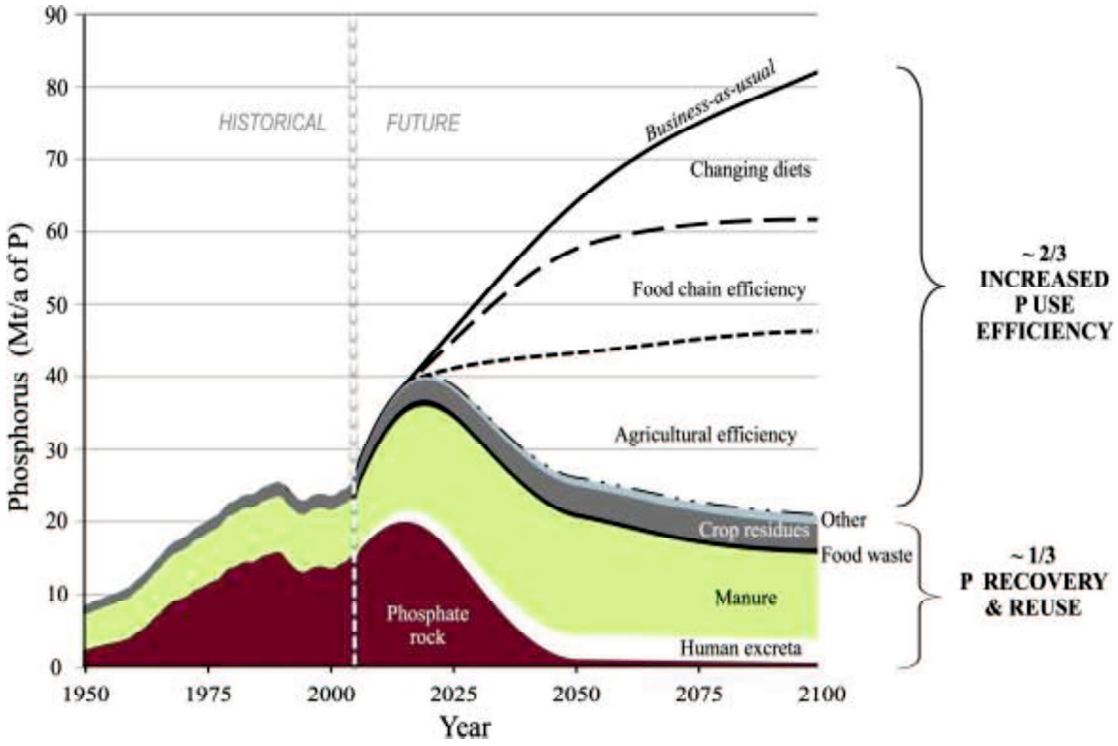

Fig. 2-1 A sustainable scenario for meeting long-term future phosphorus demand through phosphorus use efficiency and recovery.

2.2 Phosphorus removal technologies

The development of technology for phosphorus removal offers the opportunity for recycling and phosphorus sustainability. However, there are a number of technologies, both established and under development, which can be used to remove phosphorus from wastewater and can potentially be used within a sustainability strategy.

2.2.1 Chemical precipitation

The widespread use of chemical precipitation for phosphorus removal in wastewater treatment started in Switzerland during the 1950s, in response to the growing problem of eutrophication. This simple technology is now firmly established in many countries around the world. Chemical precipitation is in essence a physico–chemical process, comprising the addition of a divalent or trivalent metal salt to wastewater, causing precipitation of an insoluble metal phosphate that is settled out by sedimentation. The most suitable metals are iron (Sakadevan and Bavor, 1998, Baker et al, 1998, Seida and Nakano, 2002) and aluminium (Galarneau and Gehr, 1997, Donnert and Salecker, 1999, Özacar and Şengil, 2003), added as chlorides or sulphates. Lime (Yi and Lo, 2003) may also be used to precipitate calcium phosphate. Anionic polymers may be used to assist solid separation.

Chemical precipitation is a very flexible approach to phosphorus removal and can be applied at several stages during wastewater treatment (Fig. 2-2). Primary precipitation is where the chemical is dosed before primary sedimentation and phosphorus removed in primary sludge. Secondary (or simultaneous) precipitation is where the chemical is dosed directly to the aeration tank of an activated sludge process and phosphate removed in secondary sludge. Tertiary treatment is where dosing follows secondary treatment and although a high-quality effluent can be produced, this approach is not generally favoured because of high chemical costs and the creation of an additional, chemical, tertiary sludge.

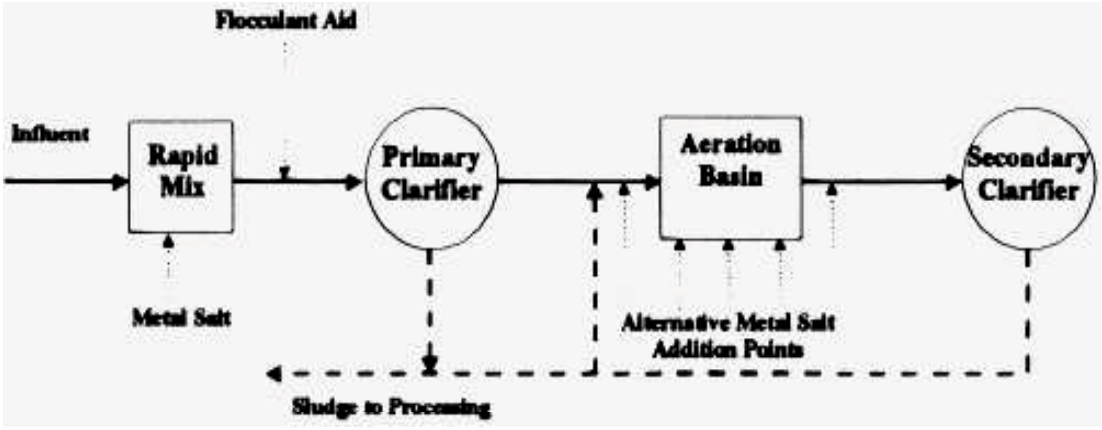

Fig. 2-2 The application of chemical precipitation.

2.2.2 Biological phosphorus removal

The development of biological phosphorus removal was based on research in the late 1950s, which found that, under certain conditions, activated sludge could take up phosphorus in considerable excess to that required for normal biomass growth (Bowker and Stensel, 1990). Biological phosphorus removal is achieved in the activated sludge process by introducing an anaerobic and/or anoxic zone ahead of an aerobic stage (Fig. 2-3). In this zone, sufficient readily degradable chemical oxygen demand (COD) must be available, typically as volatile fatty acids provided by pre-fermenting the sludge using storage or thickeners, or from the addition of acetic acid or sodium acetate. In the absence of oxygen and nitrates, bacteria, such as Acinetobacter take up the acids and release phosphorus into solution, but in the aerobic stage luxury uptake occurs, increasing overall phosphorus removal rates to as much as 80–90%. However, removal is variable and, in practice, the achievement of a low and consistent effluent standard may require complementary chemical (simultaneous) precipitation. Recently, an enhanced biological phosphorus removal (EBPR) is developed to increase the efficiency of phosphorus removal, which based on the selective enrichment of bacteria accumulating inorganic polyphosphate as an ingredient of their cells (Mino et al, 1998, Mino, 2000).

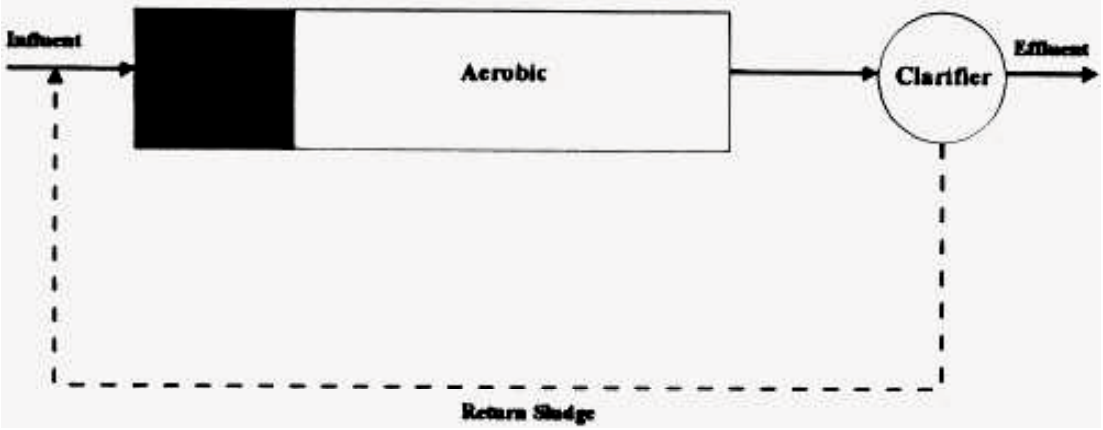

Fig. 2-3 A basic biological phosphorus removal process.

2.2.3 Crystallization technologies

The development of crystallization technology started in the 1970s, in response to more stringent phosphorus removal requirements combined with the desire to produce a more marketable end-product. Although there have been a number of initiatives, the leaders in this technology are DHV Consulting Engineers (Fig. 2-4), who adapted their expertise in water softening (Dijk and Eggers, 1987). The two main crystallization processes are the crystallization of struvite (NH_4MgPO_4–MAP) and crystallization of hydroxyapatite ($Ca_5(PO_4)_3OH$–HAP), which can be achieved with various plant configuration, such like the DHV crystalacor, the Rim-Nut ion exchange process, the Unitika Phosnix process and the Kurita fixed bed crystallization (Battistoni et al, 2001, Battistoni et al, 2002, Mehta and Batstone, 2013).

2.2.4 Adsorption

Adsorption approach is one of the most effective and economical technologies. The potential advantages are that no additional sludge is produced, reagents are not needed to overcome high alkalinity and wastewater pH is unaffected. Many types of adsorbents for phosphate removal have been investigated, which include aluminum oxide/hydroxides (Tanada et al, 2003), polymeric ligand exchanger (Zhao and Sengupta, 1998), industrial byproducts (Kostura et al, 2005), zeolite (Onyango et al, 2007), layered double hydroxides (Kuzawa et al, 2006), and so on.

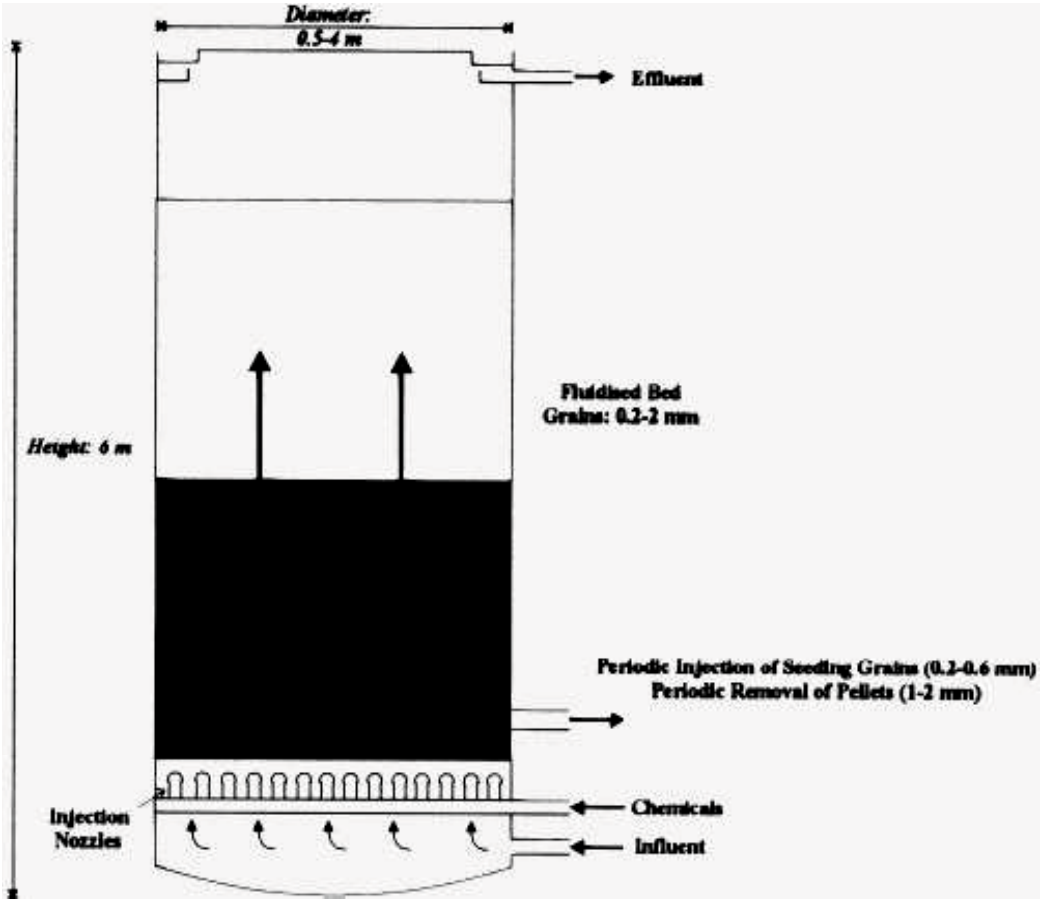

Fig. 2-4 The DHV Crystalactor™.

2.2.5 Cost calculation

The costs of upgrading facility performance include both a capital cost and an operation and maintenance (O & M) cost. The O & M cost is estimated includes components costs for energy, chemicals, sludge disposal and maintenance. A comparison based on economic cost of four alternatives are shown in Table 2-1. Chemical precipitation process performs better in terms of effluent quality, however high chemicals consumption such as iron, aluminum and their hydroxide are required as well as a great number of chemical sludge are produced. Biological phosphorus removal process almost do not need any chemicals, instead, it requires more energy and construction volume in order for aeration device. Crystallization process could provide a marketable end-production such as phosphate fertilizer, however medium chemicals are need, in additional, the crystallization process should be keep strictly in

high pH value, which means life of device is shorten. Generally, adsorption process could be conducted under neutral condition without pH adjustment. Besides, no sludge is produced after adsorption process. Its shortcoming is that desorption and regeneration of adsorbent by using various alkaline solutions, also the disposal of these solutions after desorption, which accounts 70% of O & M cost.

Table 2-1 Comparison of cast calculation under various phosphorus removal technologies.

Items	Chemical precipitation	Biological phosphorus removal	Crystallization technologies	Adsorption
Capital costs	Low	Medium	Low	Low
Energy cost	Low	High	Low	Low
Chemicals cost	High	0	Medium	Low
Sludge production	High	Low	0	0
Maintenance	Medium	Low	Medium	Medium

2.3 Layered double hydroxides

Elevated levels of oxyanions have been found in the environment and they can be harmful to both humans and wildlife. In recent decades, a class of anionic clays known as layered double hydroxides (LDHs) or hydrotalcite-like compounds (HTLc) has attracted substantial attention from both industry and academia. Although LDHs exist as naturally occurring minerals, they are also relatively simple and economical to synthesize. The structure of LDHs is based on positively charged brucite-like sheets and the positive charges are balanced by intercalation of anions in the hydrated interlayer regions. LDHs have relatively weak interlayer bonding and, as a consequence, exhibit excellent ability to capture organic and inorganic anions. The most interesting properties of LDHs include large surface area, high anion exchange

capacity (2–3 meq/g) that is comparable to those of anion exchange resins, and good thermal stability (Bish, 1980, Cavani et al, 1991, Das et al, 2004).

LDHs have been studied for their potential use in a wide range of important areas, i.e. catalysis, photochemistry, electrochemistry, polymerization, magnetization, biomedical science, and environmental application. There has also been considerable interest in using LDHs to remove environmental contaminants since environmental pollution has emerged as an important issue in the recent decades. Significant progress has been achieved in the research and development of LDHs' application in environmental protection, such as their use as environmental catalysts in removing organic and inorganic wastes (Corma et al, 1997, Kannan, 1998, Palomares et al, 2004). LDHs have also been used as novel membrane-like materials to partition pyrene from a methanol–water solution containing the polycyclic aromatic hydrocarbon (Dutta and Robins, 1994). Indeed, increasing interest has recently been diverted to evaluating the ability of LDHs to remove inorganic contaminants such as oxyanions (e.g. arsenite, arsenate, chromate, phosphate, selenite, selenate, borate, nitrate, etc.) and monoatomic anions (e.g. fluoride, chloride, bromide, and iodide) from aqueous solutions by the process of adsorption and ion exchange. This is because LDHs have exhibited a great potential to efficiently remove harmful oxyanions due to their superior characteristics.

2.3.1 Composition and structure of LDHs

LDHs are a class of two-dimensional nanostructured anionic clays. The structure of LDHs can be described as a cadmium iodide-type layered hydroxide (e.g., brucite, $Mg(OH)_2$), where a fraction of the divalent cations coordinated octahedrally by hydroxyl groups have been isomorphously replaced by trivalent cations, giving positively charged sheets. The net positive charge is compensated by anions in the interlayer region between the brucite-like sheets. Some hydrogen-bonded water molecules may occupy the free space in this interlayer region. The structure of LDHs and a typical octahedral unit are shown in (Fig. 2-5). The basal spacing (c') is the

total thickness of the brucite-like sheet and the interlayer region. The octahedral units of M^{2+} or M^{3+} (sixfold coordinated to OH^-) share edges to form infinite sheets. These sheets are stacked on top of each other and are held together by hydrogen bonding.

LDHs can be represented by the general formula $[M_{1-x}^{2+}M_x^{3+}(OH)_2]^{x+}(A^{n-})_{x/n}\cdot mH_2O$, where M^{2+} and M^{3+} are divalent and trivalent cations, respectively; the value of x is equal to the molar ratio of $M^{3+}/(M^{2+}+M^{3+})$, whereas A is the interlayer anion of valence n. The identities of M^{2+}, M^{3+}, x, and A^{n-} may vary over a wide range, thus giving rise to a large class of isostructural materials with varied physicochemical properties(Evans and Duan, 2006). The parent material of these anionic clays is the naturally occurring mineral hydrotalcite which has the formula $Mg_6Al_2(OH)_{16}CO_3\cdot 4H_2O$.

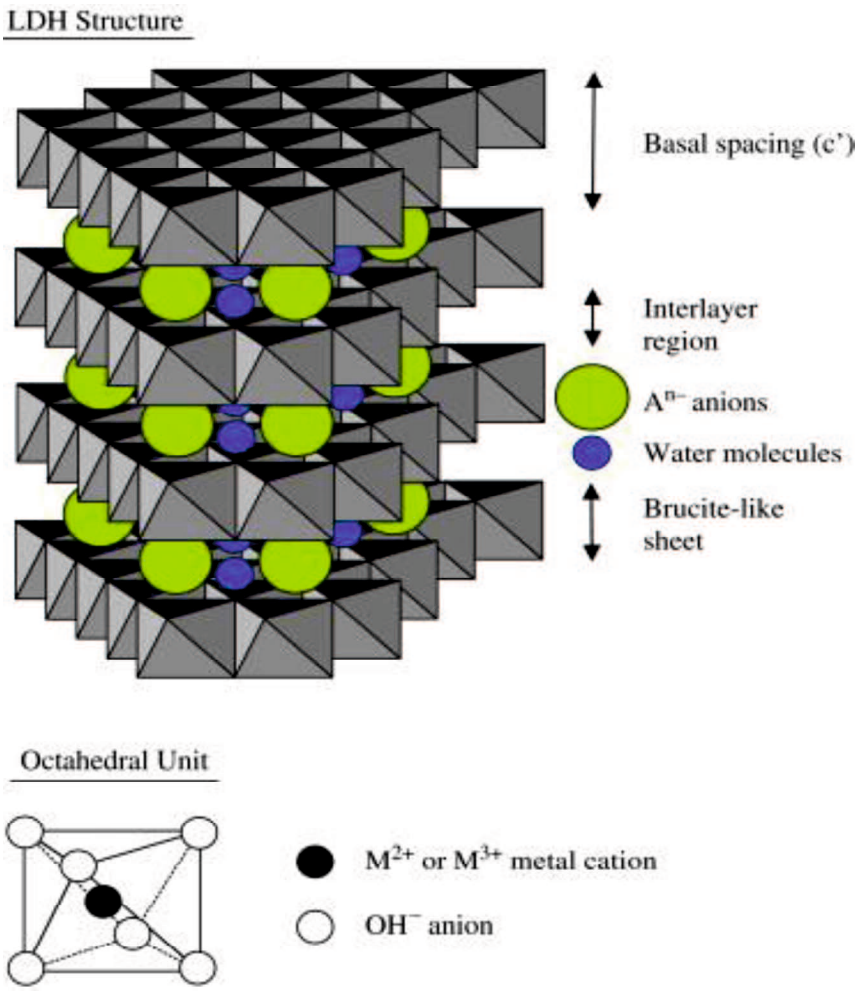

Fig. 2-5 Schematic representation of the LDH structure.

2.3.2 Synthesis of LDHs

LDHs can be regarded as a class of materials that are simple to synthesize in the laboratory, although not always as pure phases. In general, there are several approaches to prepare LDHs which including coprecipitation methods, ion exchange methods, hydrothermal methods and the others (He et al, 2006).

2.3.3 Characterization of LDHs

A wide range of analytical techniques have been used to characterize LDHs. The routine analyses that are most frequently used are powder X-ray diffraction (XRD), Fourier transform infrared spectroscopy (FTIR), and Raman spectroscopy. Other routine analyses include thermogravimetry (TG), differential scanning calorimetry (DSC), differential thermal analysis (DTA), scanning electron microscopy (SEM), and transmission electron microscopy (TEM).

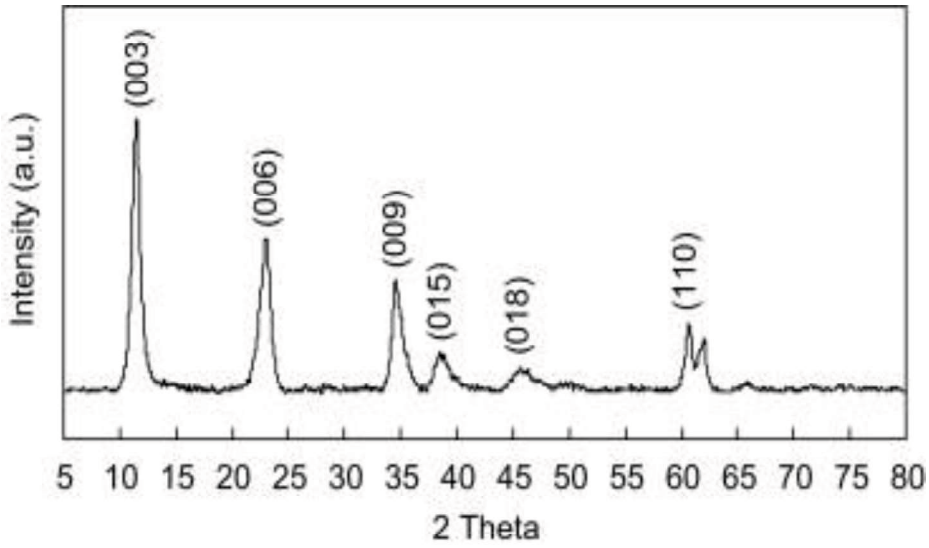

Fig. 2-6 Typical X-ray pattern of LDHs.

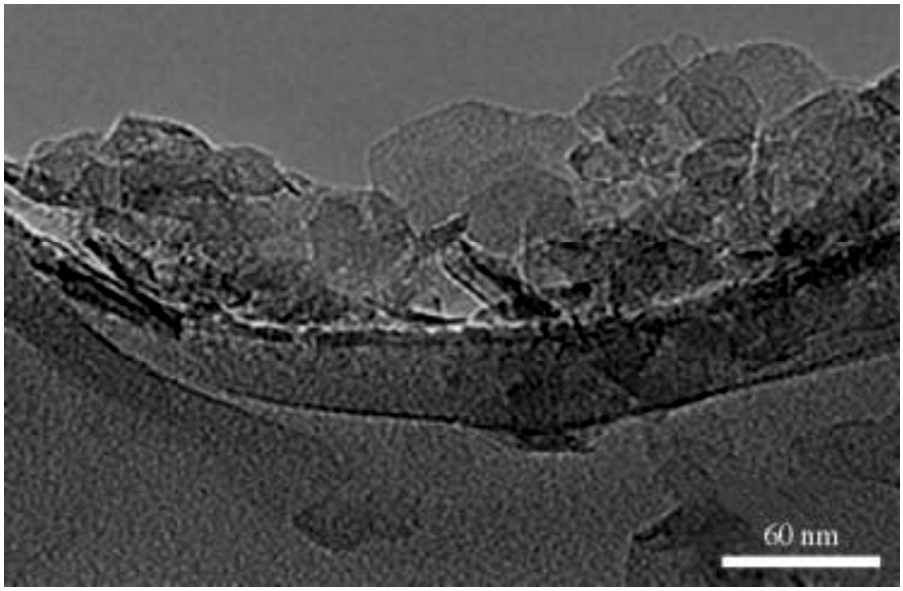

Fig. 2-7 TEM image of synthesized LDHs.

2.3.4 Adsorption of oxyanions on LDHs

In addition to the large surface area and high anion exchange capacity of LDHs, their flexible interlayer region that is accessible to various anionic species as well as polar molecular species is another important feature promising their high removal efficiencies of contaminants. In the past few years, many reports on adsorption of various contaminants on LDHs have been published. The contaminants include oxyanions, monoatomic anions, cations, organics, and gas.

Thus far, the oxyanions investigated are arsenite (H_3AsO_3 or $H_2AsO_3^-$), arsenate ($HAsO_4^{2-}$ or AsO_4^{3-}), chromate (CrO_4^{2-} or $Cr_2O_7^{2-}$), phosphate (PO_4^{3-}), selenite ($HSeO_3^-$ or SeO_3^{2-}), selenate ($HSeO_4^-$ or SeO_4^{2-}), borate (BO_3^{3-}), nitrate (NO_3^-), perrhenate (ReO_4^-), pertechnetate (TcO_4^-), iodate (IO_3^-), molybdate (MoO_4^{2-}), and vanadate (VO_4^{3-}). The ionic radius of the oxyanions listed falls in the range of 0.19–0.26 nm. The ion exchange would reach its maximum when the interlayer region is large enough for the oxyanions to fit into the region for exchange process. The list of oxyanions which have been investigated for their adsorption characteristics with various LDHs is presented in Table 2-1.

Table 2-2 List of oxyanions investigated for their adsorption characteristics with various LDHs.

Oxyanion	Types of LDHs	Reference
Arsenite	Uncalcined carbonate-LDHs	(Manju and Anirudhan, 2000)
Arsenite	Uncalcined and calcined Mg-Al LDHs	(Yang et al, 2005)
Arsenate	Calcined Mg-Al LDHs	(Yang et al, 2006)
Arsenate	Uncalcined chloride-Li-Al LDHs	(Liu et al, 2006)
Chromate	Uncalcined Mg-Fe LDHs	(Das,Das, 2004)
Chromate	Uncalcined Li-Al LDHs	(Wang et al, 2006)
Phosphate	Calcined Mg-Mn LDHs	(Chitrakar et al, 2005)
Phosphate	Uncalcined and calcined Mg-Al, Zn-Al, Ni-Al, Co-Al, Mg-Fe, Zn-Fe, Ni-Fe, and Co-Fe LDHs	(Das et al, 2006)
Selenite	Uncalcined Mg-Fe LDHs	(Das et al, 2002)
Selenite	Uncalcined and calcined LDHs	(Yang,Shahrivari, 2005)
Selenate	Uncalcined choride-Mg-Al and chloride-Zn-Al LDHs	(You et al, 2001)
Selenate	Uncalcined hydroxide-Ca-Al LDHs and carbonate-Ca-Al LDHs	(Zhang and Reardon, 2003)
Borate	Uncalcined Mg-Al and Mg-Fe LDHs	(Ferreira et al, 2006)
Borate	Uncalcined and calcined nitrate-Mg-Al LDHs	(Ay et al, 2007)
Nitrate	Uncalcined chloride-Mg-Al, Co-Fe, Ni-Fe, and Mg-Fe LDHs	(Tezuka et al, 2004)
Nitrate	Uncalcined Zn-Al LDHs	(Frost and Musumeci, 2006)
Perrhenate	Calcined Mg-Al LDHs	(Kang et al, 1999)
Perrhechnetate	Uncalcined M(Ⅱ)-M(Ⅲ) LDHs	(Wang and Gao, 2006)
Idate	Uncalcined carbonate-Mg-Al LDHs	(Toraishi et al, 2002)

	and nitrate-Mg-Al LDHs	
Molybdate	Uncalcined hydroxide-Ca-Al LDHs and carbonate-Ca-Al LDHs	(Zhang and Reardon, 2003)
Vanadate	Calcined Mg-Al LDHs	(Kovanda et al, 1999)

2.3.5 Mechanism studies

Mechanistic study of oxyanion adsorption is of paramount importance in the understanding of the adsorbate–adsorbent interaction, which can lead to the optimization of the adsorption process and the subsequent desorption/regeneration process. Recently, (Wang,Hseu, 2006) developed a mechanistic model to describe the adsorption and desorption of Cr(VI) on/from chloride-Li–Al LDHs (Fig. 2-8) in four steps:

1) In Step 1, Cr(VI) in the solution is adsorbed rapidly through ion exchange, and the Cl^- on the surface of LDHs or at the edge of the interlayer is replaced by the adsorbed Cr(VI).

2) In Step 2, the Cl^- at the edge of the interlayer and the Li^+ from the brucite-like sheets start diffusing out to the bulk solution.

3) In Step 3, the deintercalation of Li–Al LDHs due to the increasing release of Li^+ results in the desorption of both Cr(VI) (on the basal surfaces and/or edges of LDHs) and Cl^- (in the interlayers).

4) In Step 4, the desorption rate of the Cr(VI) gradually decreases until the reaction reaches equilibrium.

However, the mechanism of phosphate adsorption by LDHs has not been thoroughly studied in detail so far. Because both phosphate and chromate are oxyanion, i suppose that their adsorption mechanisms are similar which attribute to ion exchange process.

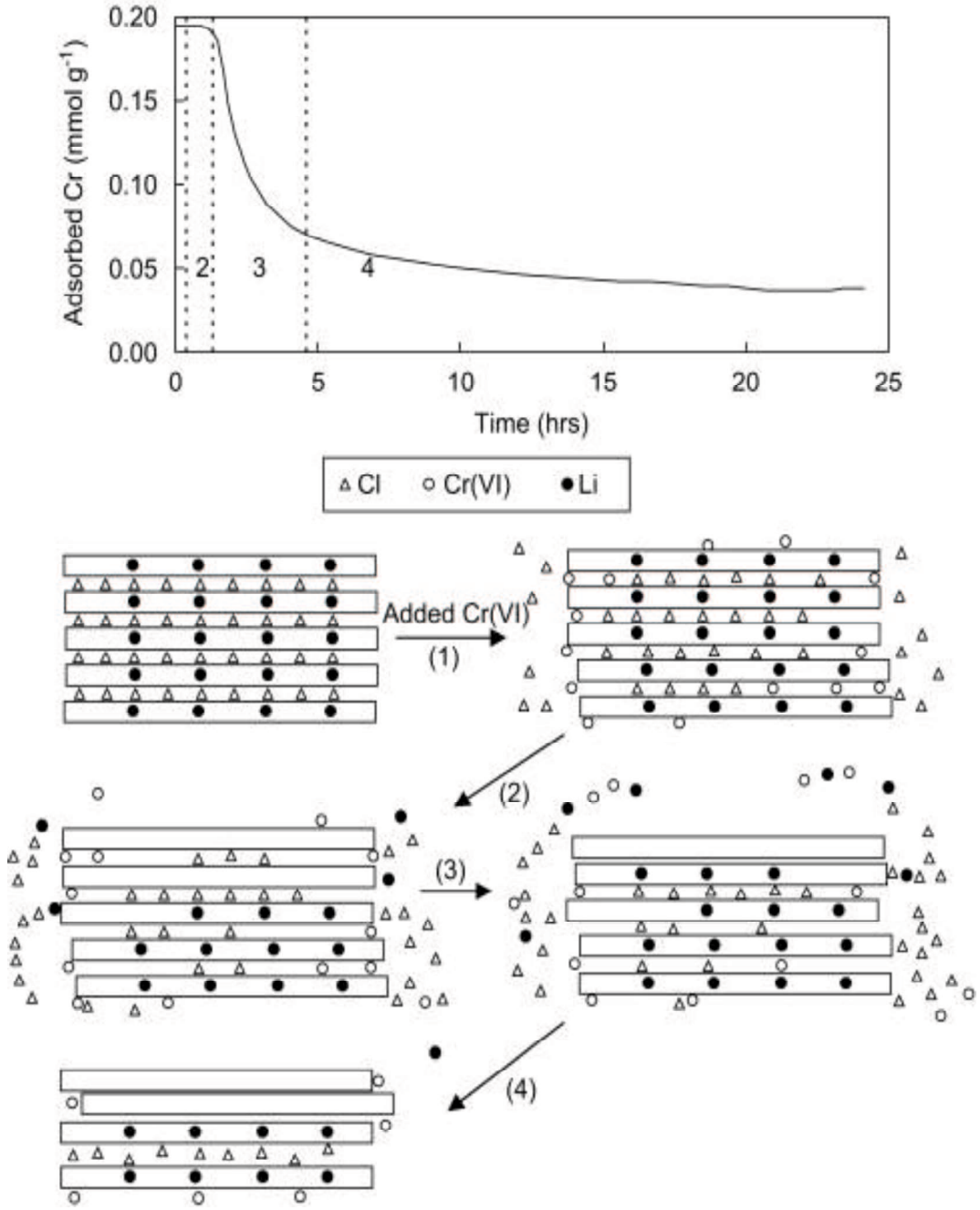

Fig. 2-8 A proposed mechanism for the adsorption and desorption of Cr(VI) in Li–Al LDHs.

2.4 Reference

Ay, A.N., B. Zümreoglu-Karan, and A. Temel. 2007. Boron removal by hydrotalcite-like, carbonate-free Mg-Al-NO3-LDH and a rationale on the mechanism. *Microporous and Mesoporous Materials*, **98**(1-3), 1-5.

Baker, M.J., D.W. Blowes, and C.J. Ptacek. 1998. Laboratory development of permeable reactive mixtures for the removal of phosphorus from onsite wastewater disposal systems. *Environmental Science and Technology*, **32**(15), 2308-2316.

Battistoni, P., A. De Angelis, P. Pavan, M. Prisciandaro, and F. Cecchi. 2001. Phosphorus removal from a real anaerobic supernatant by struvite crystallization. *Water Research*, **35**(9), 2167-2178.

Battistoni, P., A. De Angelis, M. Prisciandaro, R. Boccadoro, and D. Bolzonella. 2002. P removal from anaerobic supernatants by struvite crystallization: long term validation and process modelling. *Water Research*, **36**(8), 1927-1938.

Bish, D.L. 1980. Anion-exchange in takovite: applications to other hydroxide minerals. *Bulletin de Mineralogie*, **103**(170-175.

Bowker, R.P.G. and H.D. Stensel. 1990. *Phosphorus Removal from Wastewater*,

Cavani, F., F. Trifirò, and A. Vaccari. 1991. Hydrotalcite-type anionic clays: Preparation, properties and applications. *Catalysis Today*, **11**(2), 173-301.

Chitrakar, R., S. Tezuka, A. Sonoda, K. Sakane, K. Ooi, and T. Hirotsu. 2005. Adsorption of phosphate from seawater on calcined MgMn-layered double hydroxides. *Journal of Colloid and Interface Science*, **290**(1), 45-51.

Cordell, D., J.O. Drangert, and S. White. 2009. The story of phosphorus: Global food security and food for thought. *Global Environmental Change*, **19**(2), 292-305.

Cordell, D., S. White, J.O. Drangert, and T.S.S. Neset. 2009. Preferred future phosphorus scenarios: A framework for meeting long-term phosphorus needs for global food demand. *International Conference on Nutrient Recovery from Wastewater Streams Vancouver, 2009*,

Corma, A., A.E. Palomares, F. Rey, and F. Márquez. 1997. Simultaneous catalytic removal of SOx and NOx with hydrotalcite-derived mixed oxides containing copper, and their possibilities to be used in FCC units. *Journal of Catalysis*, **170**(1), 140-149.

Déry, P. and B. Anderson. 2007.

Das, J., D. Das, G.P. Dash, D.P. Das, and K. Parida. 2004. Studies on Mg/Fe hydrotalcite-like - Compound (HTlc): Removal of chromium (VI) from aqueous solution. *International Journal of Environmental Studies*, **61**(5), 605-616.

Das, J., D. Das, G.P. Dash, and K.M. Parida. 2002. Studies on Mg/Fe hydrotalcite-like-compound (HTlc): I. Removal of inorganic selenite (SeO3 2-) from aqueous medium. *Journal of Colloid and Interface Science*, **251**(1), 26-32.

Das, J., B.S. Patra, N. Baliarsingh, and K.M. Parida. 2006. Adsorption of phosphate by layered double hydroxides in aqueous solutions. *Applied Clay Science*, **32**(3-4), 252-260.

Dijk, J.C. and E. Eggers. 1987. Removal of phosphate at sewage treatment plants in a fluidised bed rector. *H₂O*, **20**(3), 63-68.

Donnert, D. and M. Salecker. 1999. Elimination of phosphorus from municipal and industrial waste water. *Water Science and Technology*, **40**(4–5), 195-202.

Dutta, P.K. and D.S. Robins. 1994. Pyrene sorption in organic-layered double-metal hydroxides.

Langmuir, **10**(6), 1851-1856.

Evans, D.G. and X. Duan. 2006. Preparation of layered double hydroxides and their applications as additives in polymers, as precursors to magnetic materials and in biology and medicine. *Chemical Communications (Cambridge, United Kingdom)*, 5), 485-496.

Ferreira, O.P., S.G. De Moraes, N. Durán, L. Cornejo, and O.L. Alves. 2006. Evaluation of boron removal from water by hydrotalcite-like compounds. *Chemosphere*, **62**(1), 80-88.

Frost, R.L. and A.W. Musumeci. 2006. Nitrate absorption through hydrotalcite reformation. *Journal of Colloid and Interface Science*, **302**(1), 203-206.

Galarneau, E. and R. Gehr. 1997. Phosphorus removal from wastewaters: Experimental and theoretical support for alternative mechanisms. *Water Research*, **31**(2), 328-338.

He, J., M. Wei, B. Li, Y. Kang, D. Evans, and X. Duan. 2006 *Preparation of Layered Double Hydroxides, Layered Double Hydroxides*. Springer Berlin / Heidelberg,

Heffer, P. and M. Prud'homme. 2009.

Kang, M.J., K.S. Chun, S.W. Rhee, and Y. Do. 1999. Comparison of sorption behavior of I- and TcO4 - on Mg/Al layered double hydroxide. *Radiochimica Acta*, **85**(1-2), 57-63.

Kannan, S. 1998. Decomposition of nitrous oxide over the catalysts derived from hydrotalcite-like compounds. *Applied Clay Science*, **13**(5-6), 347-362.

Kostura, B., H. Kulveitová, and J. Leško. 2005. Blast furnace slags as sorbents of phosphate from water solutions. *Water Research*, **39**(9), 1795-1802.

Kovanda, F., E. Kovácsová, and D. Koloušek. 1999. Removal of anions from solution by calcined hydrotalcite and regeneration of used sorbent in repeated calcination-rehydration-anion exchange processes. *Collection of Czechoslovak Chemical Communications*, **64**(9), 1517-1528.

Kuzawa, K., Y.-J. Jung, Y. Kiso, T. Yamada, M. Nagai, and T.-G. Lee. 2006. Phosphate removal and recovery with a synthetic hydrotalcite as an adsorbent. *Chemosphere*, **62**(1), 45-52.

Liu, Y.T., M.K. Wang, T.Y. Chen, P.N. Chiang, P.M. Huang, and J.F. Lee. 2006. Arsenale sorption on lithium/aluminum layered double hydroxide intercalated by chloride and on gibbsite: Sorption isotherms, envelopes, and spectroscopic studies. *Environmental Science and Technology*, **40**(24), 7784-7789.

Manju, G.N. and T.S. Anirudhan. 2000. Treatment of arsenic (III) containing wastewater by adsorption on hydrotalcite. *Indian Journal of Environmental Health*, **42**(1), 1-8.

Mehta, C.M. and D.J. Batstone. 2013. Nucleation and growth kinetics of struvite crystallization. *Water Research*, **47**(8), 2890-2900.

Mino, T. 2000. Microbial Selection of Polyphosphate-Accumulating Bacteria in Activated Sludge Wastewater Treatment Processes for Enhanced Biological Phosphate Removal. *Biochemistry (Moscow)*, **65**(3), 341-348.

Mino, T., M.C.M. van Loosdrecht, and J.J. Heijnen. 1998. Microbiology and biochemistry of the enhanced biological phosphate removal process. *Water Research*, **32**(11), 3193-3207.

Onyango, M.S., D. Kuchar, M. Kubota, and H. Matsuda. 2007. Adsorptive removal of phosphate ions from aqueous solution using synthetic zeolite. *Industrial and Engineering Chemistry Research*, **46**(3), 894-900.

Özacar, M. and İ.A. Şengil. 2003. Enhancing phosphate removal from wastewater by using polyelectrolytes and clay injection. *Journal of Hazardous Materials*, **100**(1–3), 131-146.

Palomares, A.E., J.G. Prato, F. Rey, and A. Corma. 2004. Using the "memory effect" of hydrotalcites for improving the catalytic reduction of nitrates in water. *Journal of Catalysis*, **221**(1), 62-66.

Rosemarin, A., G. de Bruijne, and I. Caldwell. 2009. Peak phosphorus: the next inconvenient truth. *The Broker*, **15**(6-9.

Sakadevan, K. and H.J. Bavor. 1998. Phosphate adsorption characteristics of soils, slags and zeolite to be used as substrates in constructed wetland systems. *Water Research*, **32**(2), 393-399.

Seida, Y. and Y. Nakano. 2002. Removal of phosphate by layered double hydroxides containing iron. *Water Research*, **36**(5), 1306-1312.

Smit, A.L., P.S. Bindraban, J.J. Schröder, J.G. Conijn, and H.G. van der Meer. 2009. Phosphorus in agriculture: Global resources, trends and developments. *Phosphorus in Agriculture: Global Resources, Trends and Developments*,

Tanada, S., M. Kabayama, N. Kawasaki, T. Sakiyama, T. Nakamura, M. Araki, and T. Tamura. 2003. Removal of phosphate by aluminum oxide hydroxide. *Journal of Colloid and Interface Science*, **257**(1), 135-140.

Tezuka, S., R. Chitrakar, K. Sakane, A. Sonoda, K. Ooi, and T. Tomida. 2004. The synthesis and phosphate adsorptive properties of Mg(II)-Mn(III) layered double hydroxides and their heat-treated materials. *Bulletin of the Chemical Society of Japan*, **77**(11), 2101-2107.

Toraishi, T., S. Nagasaki, and S. Tanaka. 2002. Adsorption behavior of IO3 - by CO3 2-- and NO3 --hydrotalcite. *Applied Clay Science*, **22**(1-2), 17-23.

Vaccari, D.A. 2009. Phosphorus: A looming crisis. *Scientific American*, **300**(42-47.

Wang, S.L., R.J. Hseu, R.R. Chang, P.N. Chiang, J.H. Chen, and Y.M. Tzou. 2006. Adsorption and thermal desorption of Cr(VI) on Li/Al layered double hydroxide. *Colloids and Surfaces A: Physicochemical and Engineering Aspects*, **277**(1-3), 8-14.

Wang, Y. and H. Gao. 2006. Compositional and structural control on anion sorption capability of layered double hydroxides (LDHs). *Journal of Colloid and Interface Science*, **301**(1), 19-26.

Yang, L., M. Dadwhal, Z. Shahrivari, M. Ostwal, P.K.T. Liu, M. Sahimi, and T.T. Tsotsis. 2006. Adsorption of arsenic on layered double hydroxides: Effect of the particle size. *Industrial and Engineering Chemistry Research*, **45**(13), 4742-4751.

Yang, L., Z. Shahrivari, P.K.T. Liu, M. Sahimi, and T.T. Tsotsis. 2005. Removal of trace levels of arsenic and selenium from aqueous solutions by calcined and uncalcined layered double hydroxides (LDH). *Industrial and Engineering Chemistry Research*, **44**(17), 6804-6815.

Yi, W.G. and K.V. Lo. 2003. Phosphate recovery from greenhouse wastewater. *Journal of Environmental Science and Health - Part B Pesticides, Food Contaminants, and Agricultural Wastes*, **38**(4), 501-509.

You, Y., G.F. Vance, and H. Zhao. 2001. Selenium adsorption on Mg-Al and Zn-Al layered double hydroxides. *Applied Clay Science*, **20**(1-2), 13-25.

Zhang, M. and E.J. Reardon. 2003. Removal of B, Cr, Mo, and Se from wastewater by incorporation into hydrocalumite and ettringite. *Environmental Science and Technology*, **37**(13), 2947-2952.

Zhao, D. and A.K. Sengupta. 1998. Ultimate removal of phosphate from wastewater using a new class of polymeric ion exchangers. *Water Research*, **32**(5), 1613-1625.

CHAPTER 3
ADSORPTION OF PHOSPHATE BY CALCINED MG_3-FE LAYERED DOUBLE HYDROXIDE ON BATCH EXPERIMENTS

3.1 Introduction

Phosphorus is an essential nutrient for both humans and green plants. Nevertheless, excessive discharge of phosphorus from industrial, agricultural, and household sources into rivers and lakes causes eutrophication. On the other hand, phosphorus resources are limited, and there have been some alarming reports that deposits of high-grade phosphate ores are likely to be depleted in the next few decades. Consequently, removal and recovery of phosphorus from liquid solutions is expected to be important.

Recently, numerous studies have investigated methods of removing phosphorus from waste solutions, including chemical precipitation and crystallization (de-Bashan and Bashan, 2004, Song et al, 2007), an enhanced biological phosphorus removal process (Mino et al, 1998), adsorption, and constructed wetlands. Among them, adsorption is a promising technique that is both cost effective and environmentally friendly. Layered double hydroxides (LDHs) have been paid considerable attention for their applications in removing negatively charged species through both surface adsorption and anion exchange. Their high uptake levels of anionic species can be accounted for by their large surface areas, high anion-exchange capacities, and flexible interlayer space (Li and Duan, 2006). Several factors that can influence the oxyanion adsorption by LDHs have been studied. Some researchers reported that PO_4^{3-} removal by LDHs could reach a maximum at pH 7–9 (Chitrakar et al, 2005, Das et al, 2006). Another key factor is the calcination temperature. Numerous studies

have reported that calcined LDHs were considerably more effective in removing phosphates than uncalcined ones (Lazaridis et al, 2002, Yang et al, 2005).

In the present work, we examined the phosphate adsorption performance of calcined Mg-Fe LDHs (CLDHs) using synthesized NaH_2PO_4 solution as an object of adsorption. The effects of the Mg/Fe molar ratio, influence of competitive anions, adsorption kinetics, phosphate adsorption isotherm, phosphate desorption were studied via batch tests.

3.2 Materials and methods

3.2.1 Preparation of calcined Mg-Fe LDHs

For synthesis of the calcined Mg-Fe LDH, a coprecipitation method was used under low supersaturation conditions. First, 100 ml of a mixture of 1 mol/l $MgCl_2$ and 1 mol/l $FeCl_3$ aqueous solutions with a Mg/Fe molar ratio from 0.5 to 5 was added dropwise to 250 ml of deionized water in a 500 ml beaker. A second mixture of 1 mol/l NaOH and 1 mol/l Na_2CO_3 solutions with a 3:1 volume ratio was simultaneously added into the beaker and continuously and vigorously stirred in order to maintain the pH at 10.0 ± 0.2. After the process of precipitation was completed, the suspension was aged at 353 K for 24 h in a water bath, and then the precipitate was filtered and washed thoroughly with ultrapure water until neutral (pH=7) and dried at 353 K for 24 h. The obtained Mg-Fe LDH precursor was calcined at 573 K for 3 h in a muffle furnace, then crushed and sieved into mesh sizes of 200–500.

3.2.2 Chemical analysis

The powder X-ray diffraction (XRD) patterns were obtained using an X-ray diffractometer equipped with a Ni-filtered Cu K α radiation source and a graphite monochromator. The concentration of phosphate ions in the solution phase was determined by using the vanadomolybdophosphoric acid colorimetric method. The Cl^-, NO_3^-, and SO_4^{2-} anion concentrations were determined using ion

chromatography.

3.2.3 Distribution coefficient (K_d)

For this test, 0.02 g of adsorbent sample was added to a 50 ml mixed solution of NaCl, $NaNO_3$, Na_2SO_4, and NaH_2PO_4 (0.5 mmol/L for each ion) and allowed to stand for 72 h.

The K_d values were defined as

K_d (cm^3/g) = anion adsorbed (mmol/g sample)/anion concentration in solution after equilibrium ($mmol/cm^3$).

3.2.4 Adsorption kinetics

For this test, 0.05 g of adsorbent sample was added to a 500 ml conical flask with 250 ml of synthesized NaH_2PO_4 solution and was stirred at a speed of 140 rpm at 303 K for 24 h. After the adsorption attained equilibrium, the supernatant was filtered using a 0.45 μm membrane filter to determine the phosphate concentration. The adsorption capacity of the adsorbent was calculated from the decrease in the phosphate concentration of the solution.

3.2.5 Phosphate adsorption isotherms

For this test, 0.02 g of adsorbent sample was added to 50 ml of synthesized NaH_2PO_4 with different initial phosphate concentration from 1–80 ppm and allowed to stand for 72 h to reach equilibrium.

3.2.6 Desorption studies

Before the desorption tests, 0.05 g of Mg-Fe LDH was added to 250 ml of synthesized NaH_2PO_4 solution and allowed to stand for an equilibration time of 72 h. Then, the samples were filtered using a membrane filter and washed by deionized water to remove the unabsorbed phosphate on the surfaces of the samples. Finally, 50

ml quantities of various desorption solutions were added into 300 ml conical flasks and stirred at 140 rpm for 24 h to reach equilibrium. The phosphate concentrations before and after desorption were measured.

3.3 Results and discussion

3.3.1 Effect of Mg/Fe molar ratio

In order to investigate the effect of the Mg/Fe molar ratio on the adsorption, a series of calcined and uncalcined LDHs with six different ratios from 1:2 to 5:1 was synthesized. I used a calcination temperature of 573 K, which has been confirmed by many reports (Cheng et al, 2010) to be an optimal temperature that can markedly improve the adsorption performance by eliminating CO_3^{2-} anion and water molecular in the interlayer with only slight destruction of the layered structure.

Fig. 3-1 shows that adsorption uptake by calcined LDHs was considerably higher than that of uncalcined ones for every Mg/Fe molar ratio. This result agrees with those of numerous studies (Lazaridis et al, 2001, Lazaridis,Hourzemanoglou, 2002, Álvarez-Ayuso and Nugteren, 2005). Another result observed in this figure is that similar, high phosphate adsorption capacities are obtained when the Mg/Fe molar ratio is in the range of 3–5. To explain this result, it is speculated that initially the incorporation of Fe^{3+} enhances the structural order and purity of Mg-Fe LDH when the Mg/Fe ratio increased from 0.5 to 3, while further introduction of Fe^{3+} decreases the adsorption efficiency because of the electrostatic repulsion between neighbouring trivalent metals in the layers and also the repulsion between the charge-balancing anionic interlamellar species (He et al, 2006). The most appropriate Mg/Fe ratio was 3 in both uncalcined and calcined LDHs, which agrees with observations reported by other researchers (Ferreira et al, 2004, Benselka-Hadj Abdelkader et al, 2011).

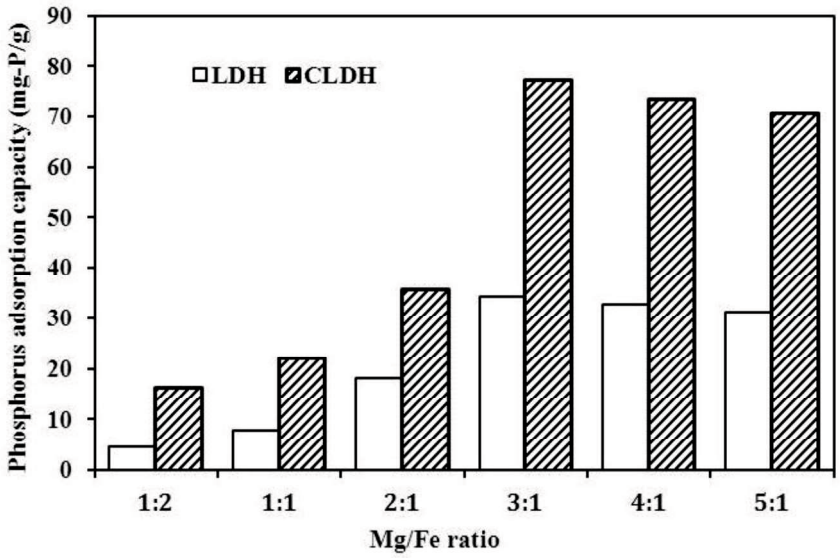

Fig. 3-1 Effect of Mg/Fe molar ratio on phosphate adsorption by LDH and CLDH.

Fig. 3-2 shows the XRD patterns of uncalcined LDHs with various Mg/Fe ratios. (003), (006), (009), (015), (018), (110) and (113) means the related plane of hexagonal unit cell in LDH which is oriented by three-dimensional coordinate axes (abc). Essentially, the reflections in the XRD pattern of an LDH fall into three groups: (1) A series of strong basal (00*l*) reflections at low angles allow direct determination of the basal spacing normal to the (00*l*) plane. (2) The position of the (110) reflection at high angle (near 60◦ 2θ for Cu) (3) Finally, the positions of the (01*l*) reflections at intermediate angles. The diffractograms have typical peaks corresponding to (003), (006), (009), (015), (018), (110) and (113) reflections at related 2θ value, which indicate the existence of the Mg-Fe LDH structure. The highest observed intensities of every typical peak in Mg_3Fe LDH reveal that highest degree of crystallinity, followed by Mg_4Fe, Mg_5Fe, Mg_2Fe, MgFe, and $MgFe_2$. This sort order is in agreement with that of the phosphate adsorption capacity. The reason that the same sort order was found even in the calcined samples could be assumed to be that the Mg_3Fe hydrotalcite also led to good reconstruction after subsequent calcination and rehydration processes (Rives and Angeles Ulibarri, 1999).

The pore structure parameters of the samples, such as specific surface area, pore volume are listed in Table 3-1. The data of sample Mg_4Fe_1 LDH and Mg_5Fe_1 LDH

were not provided because their specific surface area is too small that could not be detected by equipment. Based on available data, i concluded that among LDHs samples, Mg_3Fe_1 LDH has the largest specific surface area. After calcination, the specific surface area, pore volume were tends to increase, however, the largest specific surface area is found in sample Mg_5Fe_1 CLDH, the results were not fit with our expectation (Mg_3Fe_1 CLDH), probably due to their specific surface area is too close to distinguish with a slight experimental error.

Table 3-1 Effect of Mg/Fe molar ratio on pore structure parameters.

Samples	S_{BET} (m^2/g)	Pore volume (cm^3/g)
Mg_3Fe_1 LDH	71.77	0.122
Mg_4Fe_1 LDH	NA	NA
Mg_5Fe_1 LDH	NA	NA
Mg_3Fe_1 CLDH	80.51	0.131
Mg_4Fe_1 CLDH	77.08	0.127
Mg_5Fe_1 CLDH	88.74	0.142

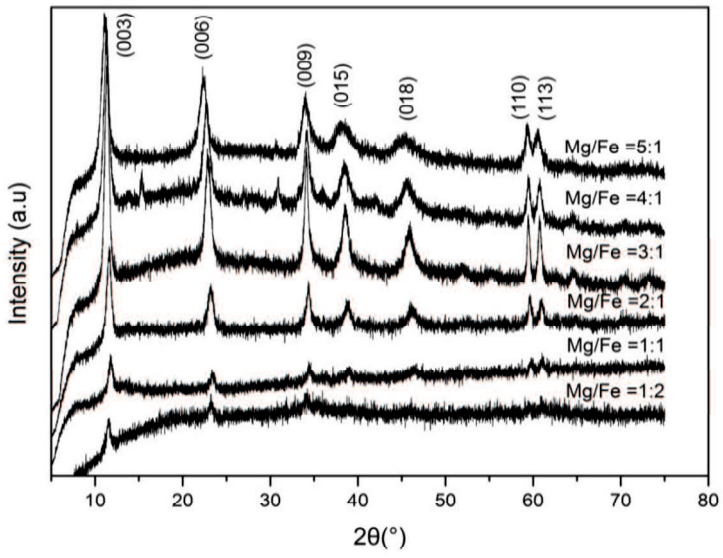

Fig. 3-2 X-ray diffraction patterns of various Mg-Fe LDHs.

3.3.2 Effect of pH

Generally pH is considered to be an important parameter that controls the adsorption at water-adsorbent interfaces. Keeping this in view, the adsorption of phosphate on calcined Mg_3Fe_1-LDH was studied at different pH values ranging from 3.8 to 10.8., which was depicted in Fig. 3-3. From the figure it may be observed that adsorption capacity increases with the increase in pH and reaches maximum at pH 6.9. With further increase in pH up to 10.8, there has been a steady decrease. This can be attributed to the increasing competition between OH^- groups and phosphate species for the adsorption sites. Phosphate exists as $H_2PO_4^-$, HPO_4^{2-} and PO_4^{3-} depending on the pH of the solution with $pK_1 = 2.15$, $pK_2 = 6.68$ and $pK_3 = 12.33$, respectively. pH 6-9 was chosen as ideal for the present study.

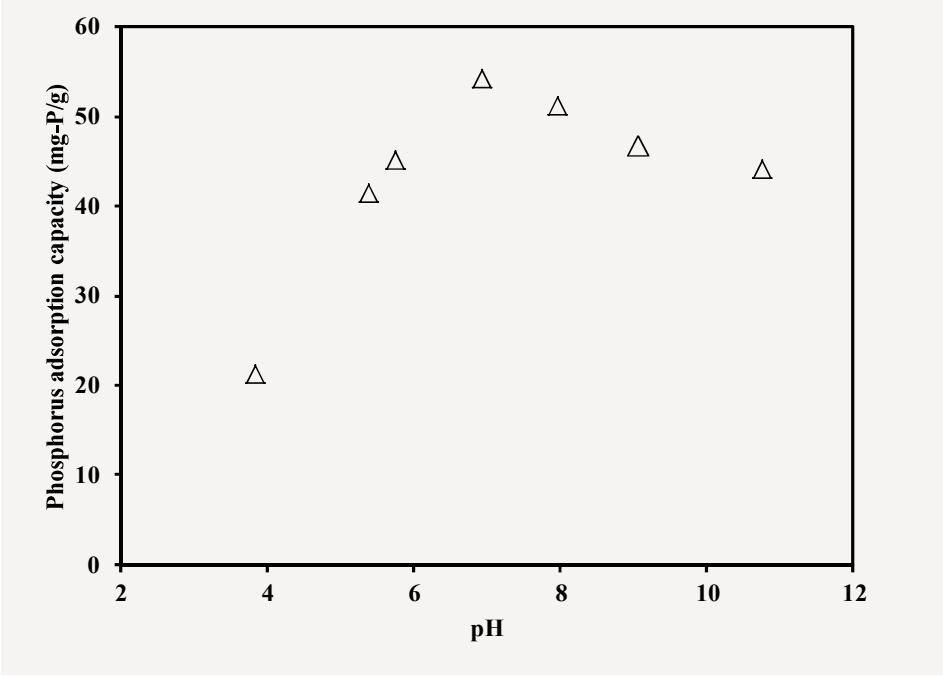

Fig. 3-3 Effect of pH on calcined Mg_3Fe_1-LDH

3.3.3 Selectivity of phosphate adsorption

Many studies have reported on the effect of competitive anions on adsorption by LDH. Depending on the pH of the solution, phosphate can exist in three different ionic species: $H_2PO_4^-$, HPO_4^{2-}, and PO_4^{3-}. When the pH of a mixed anion solution is

approximately 6.8, HPO_4^{2-} is considered to be dominant among the various ionic phosphate species in solution. In addition, Cl^-, SO_4^{2-}, and NO_3^- anions were introduced as competing ions in order to observe their effect. The coefficient values of the series of calcined and uncalcined Mg-Fe LDHs with various Mg/Fe ratios are presented in Table 3-2. The selectivity order is as follows: $HPO_4^{2-} > Cl^-$, $SO_4^{2-} > NO_3^-$, except for the Mg_1Fe_1-CLDH, for which it is $HPO_4^{2-} > SO_4^{2-} > NO_3^-$, $Cl^- \approx 0$. The Mg_3Fe_1-CLDH still had a high K_d value for phosphate, followed by Mg_4Fe_1-CLDH and Mg_5Fe_1-CLDH. The sequences of adsorption selectivity towards phosphate ion were exactly the same as the sequences of phosphate adsorption capacity observed in the foregoing discussion of effect of Mg/Fe ratios (Fig. 3-1). Furthermore, comparing the calcined Mg_3Fe_1-LDH sample with the uncalcined one, i concluded that, remarkably, calcination could not only improve adsorption capacity for phosphate anions, but also that for other anions. However the selectivity toward phosphate ions did not obviously increase.

Table 3-2 K_d values of various samples for different anions. (na: No adsorption).

Sample	K_d (cm^3/g)			
	Cl^-	NO_3^-	SO_4^{2-}	HPO_4^{2-}
Mg_1Fe_2-CLDH	6.29×10^1	na	na	1.49×10^3
Mg_1Fe_1-CLDH	na	na	8.22×10^1	2.17×10^3
Mg_2Fe_1-CLDH	7.70×10^2	9.76×10^1	2.76×10^2	4.52×10^3
Mg_3Fe_1-CLDH	1.18×10^3	3.24×10^2	9.37×10^2	6.09×10^4
Mg_4Fe_1-CLDH	7.72×10^2	2.43×10^2	8.78×10^2	3.90×10^4
Mg_5Fe_1-CLDH	5.70×10^2	na	2.00×10^2	3.02×10^4
Mg_3Fe_1-LDH	1.59×10^2	na	na	1.33×10^3

3.3.4 Adsorption kinetic studies

According to Fig. 3-4, the initial adsorption processes were very fast, occurring within 10 h, and equilibrium was reached after 3 d. Therefore, 72 h was considered to

be the equilibration time. In order to analyse the experimental results, pseudo-first-order and pseudo-second-order models were used. The adsorption kinetics was better modelled by the pseudo-second-order equation, with respect to higher coefficients of determination than the pseudo-first-order equation. The kinetic parameters evaluated on the basis of these two equations are listed together with the coefficients of determination in Table 3-3. The capacity was estimated to be 76.2 mg-P/g of adsorbent by the pseudo-second-order equation. Simultaneously, the calculated P adsorption capacity at equilibrium was 77.5 mg-P/g, which closely agree with the estimated value.

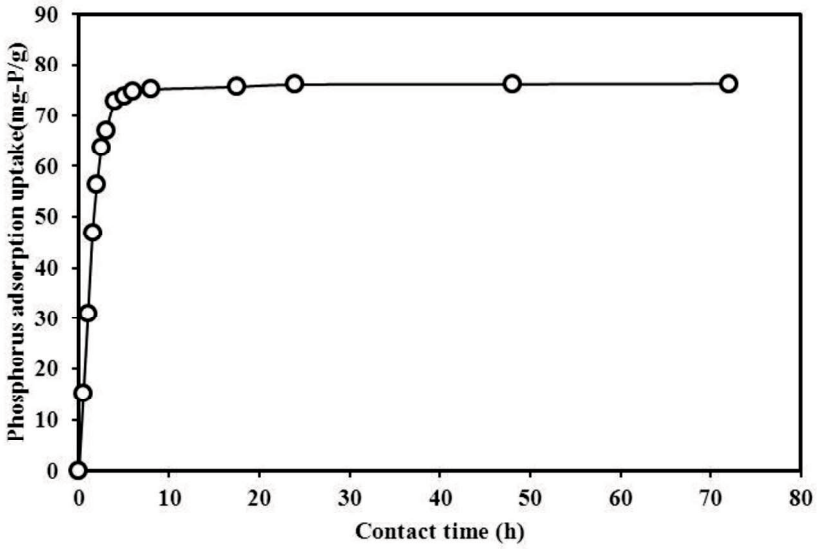

Fig. 3-4 Kinetics of phosphate adsorption on Mg_3Fe_1 CLDH.

Table 3-3 Kinetic models for adsorption on Mg_3Fe_1 CLDH and calculated constants.

Model	Equation	Mg_3Fe_1 CLDH in NaH_2PO_4 solution	
		Constant	R^2
pseudo-first-order	$\frac{dq_t}{dt} = k_1(q_e - q_t)$	$q_e = 15.30$ $k_1 = 0.320$	0.705
pseudo-second-order	$\frac{dq_t}{dt} = k_2(q_e - q_t)^2$	$q_e = 77.52$ $k_2 = 0.320$	0.999

3.3.5 Adsorption isotherm

The adsorption isotherms of phosphate ions on Mg_3Fe_1 CLDH in NaH_2PO_4 solution are presented in Fig. 3-5 from triplicate experiments. The equilibration time was determined to be 72 h in the previous section on kinetics studies. The amount of adsorption increased with increasing equilibrium concentration and reached the maximum adsorption capacity of around 150 mg-P/g when equilibrium concentration was around 30mg/L.

The Langmuir and Freundlich models are the most frequently employed models for the adsorption isotherm. In this work, both models were used to describe the adsorption isotherm.

The linear form of the Langmuir isotherm model is represented as

$$\frac{C_e}{q_e} = \frac{1}{bq_m} + \frac{C_e}{q_m}$$

where C_e is the phosphate concentration at equilibrium, q_e is the amount of adsorption at equilibrium, and q_m and b are constants related to the maximum adsorption capacity and the energy of adsorption, respectively.

The linear form of Freundlich isotherm model is represented as

$$\ln q_e = \ln K_f + \frac{1}{n} \ln C_e$$

where K_f and n are constants related to the adsorption capacity and adsorption intensity, respectively.

Comparing the coefficients of determination (R^2) listed in Table 3-4, the difference between them was statistical significant ($p < 0.05$) according to the Two Sample Paired t-Test, so it is concluded that the phosphate adsorption process was better fit with the Freundlich model than with Langmuir model.

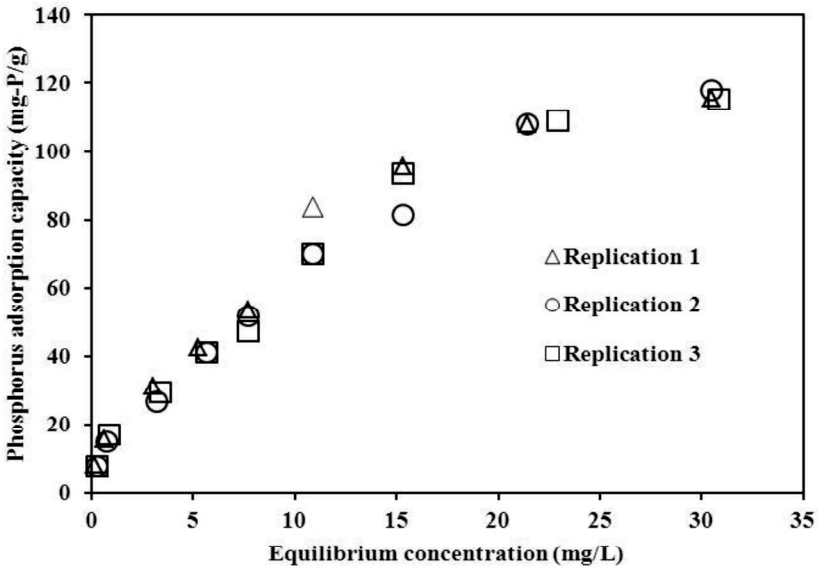

Fig. 3-5 Adsorption isotherms on Mg_3Fe_1 CLDH in triplicate.

Table 3-4 Adsorption isotherm models for adsorption on Mg_3Fe_1 CLDH and calculated constants (n=3).

Adsorbate	Langmuir model			Freundlich model		
	q_m	b	R^2	K_f	N	R^2
NaH_2PO_4 solution	156.675	0.097	0.882	17.170	1.566	0.988
	±4.871	±0.016	±0.015	±1.599	±0.287	±0.002

3.3.6 Desorption study

Various alkaline solutions, salt solutions, and mixtures thereof have been used to achieve satisfactory desorption from Mg_3Fe_1 CLDH. A series of phosphate desorption tests was carried out by using different concentrations of NaOH solutions, NaCl solutions, and mixtures thereof, as shown in Table 3-5. The NaOH solution was much more effective in desorbing phosphate ions from Mg_3Fe_1 CLDH: the desorption efficiency increased to 73.4 % when the concentration of NaOH solution increased to 0.1 M and did not obviously increase with further concentration increases, even when the concentration was increased to 1 M. The reason that an incomplete desorption process achieved was presumably the small fraction of adsorbed phosphate which was bound through strong interaction in the interlayer (Anirudhan et al, 2006). In addition,

the mixed solution did not produce better desorption efficiency, as expected, and was lower than when only NaOH solution was used. It was considered that the relatively low affinity of Cl^- to LDHs comparing with OH^- but still partial Cl^- could exchange with PO_4^{3-} anion in the interlayer (Cheng et al, 2009). Overall, based on the balance between cost savings and desorption efficiency, 0.1 M NaOH solution was chosen as the appropriate desorption solution.

A comparison of phosphate adsorption and desorption capacities of Mg_3Fe_1CLDH with various adsorbents such as carbon-based material, silica, waste material, zeolite and other LDHs was presented in Table 3-6. Among the different adsorbents, the sample synthesised in our research showed high phosphate uptake from NaH_2PO_4 solution and satisfactory desorption rate.

Table 3-5 Various desorption solutions and their desorption rates.

Desorption solution	**Desorption rate (%)**
0.01 M NaOH	34.5
0.05 M NaOH	54.1
0.1 M NaOH	73.4
0.5 M NaOH	75.8
1 M NaOH	76.4
0.05 M NaCl	10.7
0.1 M NaCl	20.9
0.5 M NaCl	28.7
1 M NaCl	35.4
0.1 M NaOH+1 M NaCl	48.7

Table 3-6 Comparison of Mg_3Fe_1CLDH with various adsorbents.

Adsorbent	Adsorption capacity (mg-P/g)	Desorption rate (%)	Reference
Mg_3Fe_1CLDH	78	73 (after 1 circle)	(Present study)
$ZnCl_2$-activated coir pith carbon	1.7	50 (after 1 circle)	(Namasivayam and Sangeetha, 2004)
Ammonium-functionalized MCM-48	15	94(after 5 circle)	(Saad et al, 2007)
Weak anion exchanger prepared from lignocellulosic residue	24	87(after 4 circle)	(Anirudhan,Noeline, 2006)
Zeolite	26	56(after 1 circle)	(Onyango et al, 2007)
Zn_2Al_1CLDH	41	-	(Cheng,Huang, 2010)

3.4 Conclusions

A calcination process at 573 K the improved phosphate adsorption capacity remarkably because of the rehydration and reconstruction of the calcined Mg-Fe LDH. The highest phosphate adsorption capacity was obtained for a sample with a Mg/Fe ratio of 3 calcined at 573 K under pH =6.9. The distribution coefficient (K_d) revealed good adsorption selectivity of Mg_3Fe_1 CLDH for phosphate in a mixed solution with NaCl, $NaNO_3$, and Na_2SO_4. The adsorption kinetics, which were studied using a pseudo-second-order model, showed high adsorption capacities of 77.5 mg-P/g in NaH_2PO_4 solution. The adsorption isotherms showed that the phosphate uptake process was better fit with the Freundlich model than with the Langmuir model. The adsorbed phosphate can be effectively desorbed (73 %) by addition of a 0.1 M NaOH solution.

3.5 Reference

Álvarez-Ayuso, E. and H.W. Nugteren. 2005. Purification of chromium(VI) finishing wastewaters using calcined and uncalcined Mg-Al-CO3-hydrotalcite. *Water Research*, **39**(12), 2535-2542.

Anirudhan, T.S., B.F. Noeline, and D.M. Manohar. 2006. Phosphate Removal from Wastewaters Using a Weak Anion Exchanger Prepared from a Lignocellulosic Residue. *Environmental Science & Technology*, **40**(8), 2740-2745.

Benselka-Hadj Abdelkader, N., A. Bentouami, Z. Derriche, N. Bettahar, and L.C. de Ménorval. 2011. Synthesis and characterization of Mg–Fe layer double hydroxides and its application on adsorption of Orange G from aqueous solution. *Chemical Engineering Journal*, **169**(1–3), 231-238.

Cheng, X., X. Huang, X. Wang, and D. Sun. 2010. Influence of calcination on the adsorptive removal of phosphate by Zn-Al layered double hydroxides from excess sludge liquor. *Journal of Hazardous Materials*, **177**(1-3), 516-523.

Cheng, X., X. Huang, X. Wang, B. Zhao, A. Chen, and D. Sun. 2009. Phosphate adsorption from sewage sludge filtrate using zinc–aluminum layered double hydroxides. *Journal of Hazardous Materials*, **169**(1-3), 958-964.

Chitrakar, R., S. Tezuka, A. Sonoda, K. Sakane, K. Ooi, and T. Hirotsu. 2005. Adsorption of phosphate from seawater on calcined MgMn-layered double hydroxides. *Journal of Colloid and Interface Science*, **290**(1), 45-51.

Das, J., B.S. Patra, N. Baliarsingh, and K.M. Parida. 2006. Adsorption of phosphate by layered double hydroxides in aqueous solutions. *Applied Clay Science*, **32**(3-4), 252-260.

de-Bashan, L.E. and Y. Bashan. 2004. Recent advances in removing phosphorus from wastewater and its future use as fertilizer (1997–2003). *Water Research*, **38**(19), 4222-4246.

Ferreira, O.P., O.L. Alves, D.X. Gouveia, A.G. Souza Filho, J.A.C. de Paiva, and J.M. Filho. 2004. Thermal decomposition and structural reconstruction effect on Mg–Fe-based hydrotalcite compounds. *Journal of Solid State Chemistry*, **177**(9), 3058-3069.

He, J., M. Wei, B. Li, Y. Kang, D. Evans, and X. Duan. 2006 *Preparation of Layered Double Hydroxides, Layered Double Hydroxides*. Springer Berlin / Heidelberg,

Lazaridis, N.K., A. Hourzemanoglou, and K.A. Matis. 2002. Flotation of metal-loaded clay anion exchangers. Part II: the case of arsenates. *Chemosphere*, **47**(3), 319-324.

Lazaridis, N.K., K.A. Matis, and M. Webb. 2001. Flotation of metal-loaded clay anion exchangers. Part I: the case of chromates. *Chemosphere*, **42**(4), 373-378.

Li, F. and X. Duan. 2006 *Applications of Layered Double Hydroxides, Layered Double Hydroxides*. Springer Heidelberg.

Mino, T., M.C.M. van Loosdrecht, and J.J. Heijnen. 1998. Microbiology and biochemistry of the enhanced biological phosphate removal process. *Water Research*, **32**(11), 3193-3207.

Namasivayam, C. and D. Sangeetha. 2004. Equilibrium and kinetic studies of adsorption of phosphate onto ZnCl2 activated coir pith carbon. *Journal of Colloid and Interface Science*, **280**(2), 359-365.

Onyango, M.S., D. Kuchar, M. Kubota, and H. Matsuda. 2007. Adsorptive removal of phosphate ions from aqueous solution using synthetic zeolite. *Industrial and Engineering Chemistry Research*, **46**(3), 894-900.

Rives, V. and M.a. Angeles Ulibarri. 1999. Layered double hydroxides (LDH) intercalated with metal coordination compounds and oxometalates. *Coordination Chemistry Reviews*, **181**(1), 61-120.

Saad, R., K. Belkacemi, and S. Hamoudi. 2007. Adsorption of phosphate and nitrate anions on ammonium-functionalized MCM-48: Effects of experimental conditions. *Journal of Colloid and Interface Science*, **311**(2), 375-381.

Song, Y., P. Yuan, B. Zheng, J. Peng, F. Yuan, and Y. Gao. 2007. Nutrients removal and recovery by crystallization of magnesium ammonium phosphate from synthetic swine wastewater. *Chemosphere*, **69**(2), 319-324.

Yang, L., Z. Shahrivari, P.K.T. Liu, M. Sahimi, and T.T. Tsotsis. 2005. Removal of trace levels of arsenic and selenium from aqueous solutions by calcined and uncalcined layered double hydroxides (LDH). *Industrial and Engineering Chemistry Research*, **44**(17), 6804-6815.

CHAPTER 4
ADSORPTION OF PHOSPHATE BY CALCINED MG_3-FE LAYERED DOUBLE HYDROXIDE ON CONTINUOUS EXPERIMENTS

4.1 Introduction

Phosphorus is an essential nutrient among plants and animals, but it is a non-renewable resource, and the global commercial phosphate reserves will be depleted in 50–100 years (Cordell et al, 2009). In recent years, the economic developments of emerging countries, such as China and India, and increasing global cereal production to cater to the biofuel boom have driven up fertilizer prices. The price of phosphorus in international trade has been driven up because of the impact of export controls in major countries of origin during the past few years (Cordell,Drangert, 2009). Japan, India, Western European nations, and many other countries lack phosphorus ore as a natural resource; thus, they completely depend on imports, and there are concerns about ensuring long-term and stable availability of phosphorus resources from recovery processes in the future. It is estimated that the amount of phosphorus contained in wastewater and sewage systems, which corresponds to 40–50% of phosphorus ore, are not utilized effectively in Japan. In a conventional, secondary, biological wastewater treatment train, some of the supernatant from the anaerobic digestion tank is recycled into the wastewater stream when primary, secondary, and waste-activated sludge are treated by anaerobic digestion (Richard, 1991). This supernatant is always rich in phosphates because they are released from phosphorus accumulation processes in microorganisms that convert the sludge solids to liquid under anaerobic conditions. Therefore, sludge can be a feasible resource for phosphorus recovery.

Recently, numerous studies have investigated methods to remove phosphorus from aqueous solutions, which include chemical precipitation and crystallization (de-Bashan and Bashan, 2004, Song et al, 2007), an enhanced biological phosphorus removal process (Mino et al, 1998), adsorption, and constructed wetlands. Among these methods, adsorption is a promising technique that is both cost effective and environmentally friendly. Layered double hydroxides (LDHs) are a class of anionic clays that have received considerable attention for their applications in removing negatively charged species via both surface adsorption and anion exchange. LDHs can be represented by the general formula $[M_{1-x}^{2+}M_x^{3+}(OH)_2]^{x+}(A^{n-})_{x/n}\text{-}mH_2O$, where M^{2+} and M^{3+} are divalent and trivalent cations, respectively; the value of x is equal to the molar ratio of $M^{3+}/(M^{2+}+M^{3+})$, and A is an interlayer anion of valence n. They are able to uptake high levels of anionic species because of their large surface areas, high anion-exchange capacities, and flexible interlayer spaces (Li and Duan, 2006). Several factors that can influence the oxyanion adsorption by LDHs have been studied. Some researchers reported that the PO_4^{3-} removal by LDHs could reach a maximum at a pH of 7–9 (Kameda et al, 2002, Chitrakar et al, 2005, Das et al, 2006), but beyond these values, the adsorption was effectively decreased as a result increasing the amount of the competing hydroxide anions. Another key factor is the calcination temperature, and several studies have reported that calcined LDHs were considerably more effective in removing phosphates than uncalcined ones (Lazaridis et al, 2002, Yang et al, 2005, Carja et al, 2005, Álvarez-Ayuso and Nugteren, 2005). The improvement was attributed to the rehydration of the calcined LDH structure when it is exposed to water and anions (memory effect) (Chibwe and Jones, 1989). The most appropriate calcination temperature was found to be 573 K (Cheng et al, 2009, Cheng et al, 2010).

During our previous work (Sun et al, 2013), a series of calcined Mg-Fe LDHs were synthesized through coprecipitation under low supersaturation conditions. Several factors that affect the adsorption process, such as Mg/Fe molar ratio, competing anions, and phosphate desorption efficiency, were studied via batch tests. However,

batch adsorption is not convenient for application on an industrial scale, in which large volumes of wastewater are continuously generated. It is imperative to analyze continuous adsorption data, which can provide valuable information for improving the design and operation of phosphate adsorption processes from wastewater treatment plants. To date, LDHs have been utilized as dispersed powders or fixed-bed granules. Granular-type adsorbents have been receiving increased attention as an alternative to powdered adsorbents because the process involving granular adsorbents is easier to control and the adsorbents are amenable to separation, especially on a continuous basis.

As a continuation of our previous work, i focused on evaluating the performance of granular calcined Mg_3-Fe LDHs for removing phosphate ions in a fixed-bed column using synthesized NaH_2PO_4 solutions. The effects of parameters such as bed-height, flow rate, and initial concentration on a breakthrough curve were investigated. Widely used column adsorption models were applied to validate the experimental data. I also assessed the performance of the granule-packed fixed-bed column in removing and recovering phosphate from actual anaerobic sludge filtrate. Finally, exhaustion-regeneration cycles were employed to investigate the reusability of the adsorbent.

4.2 Materials and methods

4.2.1 Preparation of calcined Mg_3-Fe LDH

A coprecipitation method was used under low supersaturation conditions to synthesize calcined Mg_3-Fe LDH. First, 100 mL of an aqueous solution containing 1 mol/L $MgCl_2$ and 1 mol/L $FeCl_3$ (with a Mg/Fe molar ratio of 3) was added dropwise to 250 mL of deionized water in a 500 mL beaker. A second mixture of 1 mol/L NaOH and 1 mol/L Na_2CO_3 solutions with a 3:1 volume ratio was simultaneously added into the beaker. The resultant mixture was continuously and vigorously stirred in order to maintain the pH at 10.0 ± 0.2. After the precipitation process was completed, the

suspension was aged at 353 K for 24 h in a water bath, and the precipitate was filtered and washed thoroughly with ultrapure water until neutral and dried at 353 K for 24 h. The obtained Mg_3-Fe LDH precursor was calcined at 573 K for 3 h in a muffle furnace, and subsequently crushed and sieved into mesh sizes of 200–500 mesh.

4.2.2 Chemical analysis

Powder X-ray diffraction (XRD) patterns were obtained using an X-ray diffractometer equipped with an Ni-filtered Cu Kα radiation source and a graphite monochromator (Advance D8, Bruker). The morphological features were acquired using a scanning electron microscope (SEM; JSM-6700F, JEOL). The concentration of phosphate ions in the solution phase was determined through the molybdenum blue spectrophotometric method using a spectrophotometer (U–2001, Hitachi). The Cl^-, NO_2^-, NO_3^-, and SO_4^{2-} anion concentrations were determined through ion chromatography.

4.2.3 Continuous adsorption experiments

Continuous tests were performed using transparent glass columns of inner diameter 0.05 cm and heights 6, 12, and 18 cm, respectively, for sample granules weighing 0.1, 0.2, and 0.3 g. The granules were packed into their respective columns, and synthesized NaH_2PO_4 solutions (5, 10, and 20 mg/L, respectively) or anaerobic sludge filtrate were allowed to percolate through the column from the bottom at flow rates of 12, 24, and 36 mL/h, respectively, using a peristaltic pump (SJ–1211L, ATTA). Subsequently, 100 mL of deionized water was allowed to percolate through and wash the inside of the column. Then, 0.1 M NaOH solution was used as an eluent at a flow rate of 24 mL/h. Finally, the column was washed again with 100 mL of deionized water at the same flow rate. Effluent solutions were successively collected using a fraction collector during adsorption and desorption to determine the phosphate ion concentrations. This cycle was repeated five times to investigate the reusability of the adsorbent.

For a desired initial concentration and flow rate, the value of the total mass of phosphate adsorbed, q_{total} (mg) can be calculated as being equal to the area under the plot of the adsorbed phosphate concentration:

$$q_{\mathrm{total}} = \frac{\mathrm{Q}}{1000}\int_{\mathrm{t=0}}^{\mathrm{t=total}} C_a d_t \ , \quad (1)$$

where C_a is the concentration of adsorbed phosphate (mg/L).

The equilibrium phosphate adsorption capacity, q_e (mg/g), is calculated as follows:

$$q_{\mathrm{e}} = \frac{q_{total}}{m} \ , \quad (2)$$

where m is the dosage of adsorbent packed within the column.

4.2.4 Modeling of breakthrough curves

The time or bed volume for breakthrough appearance and the shape of the breakthrough curve are important characteristics for determining the operation and dynamic response of an adsorption column (Aksu and Gönen, 2004). Furthermore, the successful design of an adsorption column requires the prediction of the concentration-time profile from the breakthrough curve for the effluent discharged from the column. In order to describe the adsorption process of phosphate on calcined Mg_3-Fe LDH absorbent, several models were introduced to fit the adsorption breakthrough curves.

The Bed Depth Service Time (BDST) Model

The BDST model (Hutchins, 1973) is based on the physical measurement of the capacity of the bed at various percentage breakthrough values. The BDST model constants can be helpful to scale up the process for other flow rates and concentrations without further experimentation. It is used to predict the column performance for any bed length, if data for some depths are known. It states that the bed depth, *Z*, and service time, t, of a column exhibit a linear relationship. The rate of adsorption is controlled by the surface reaction between the adsorbate and the unused capacity of

the adsorbent.

The BDST equation can be expressed as follows:

$$t = \frac{N_0}{C_0 U_0} Z - \frac{1}{k_a C_0} ln\left(\frac{C_0}{C} - 1\right) , \quad (3)$$

where C is the effluent concentration of a solute in the liquid phase (mg/L), C_0 is the initial concentration of the solute in the liquid phase (mg/L), U_0 is the influent linear velocity (cm/h), N_0 is the adsorption capacity (mg/g), k_a is the rate constant in the BDST model (L/ mg min), t is the time (h), and Z is the bed depth of column (cm).

A plot of t versus Z should yield a linear relationship where N_0 and k_a, which are the adsorption capacity and rate constant, respectively, can be evaluated.

The Thomas model

Predicting the concentration–time profile or breakthrough curve for the effluent is required to successfully design a column adsorption process. The maximum adsorption capacity of an adsorbent is also needed for the design. Traditionally, the Thomas model (Thomas, 1944) is used for this purpose. The model has the following form:

$$\frac{C}{C_0} = \frac{1}{1+exp[k_T(q_0 m - C_0 V_{eff})/Q]} , \quad (4)$$

where k_T is the Thomas rate constant (L/mg h), q_0 is the maximum solid-phase concentration of the solute (mg/g), m is the mass of sorbent in the column (g), V_{eff} is the throughput volume (L), and Q is the volumetric flow rate (L/h).

The Clark model

Clark (Clark, 1987) used the mass-transfer coefficient in combination with the Freundlich isotherm to define a new relation for the breakthrough curve as

$$\frac{C}{C_0} = \left(\frac{1}{1+Ae^{-rt}}\right)^{1/n-1} \quad (5)$$

with

$$A = \left(\frac{C_0^{n-1}}{C_b^{n-1}} - 1\right) e^{rt_b} \quad (6)$$

and

$$r = \frac{\beta}{U} v_m (n-1) \ , \quad (7)$$

where n is the Freundlich constant, C_b is the concentration of sorbate at breakthrough time t_b (mg/L), and ν_m is the migration velocity of the concentration front in the bed (cm/h).

The Yoon and Nelson model

The Yoon and Nelson model is a relatively simple model based on the assumption that the rate of decrease in the probability of sorption for each sorbate molecule is proportional to the probability of sorbate sorption and sorbate breakthrough on the sorbent (Yoon and Nelson, 1984). The equation for the 50% breakthrough concentration from a fixed bed of sorbent is:

$$\frac{C}{c_0 - C} = exp(k_Y t - t_{0.5} k_Y) \ , \quad (8)$$

where k_Y is the Yoon-Nelson rate constant (h^{-1}). The values of k_Y and $t_{0.5}$ can be obtained from the slope and intercept, respectively, for a linear plot of $\ln[C/(C_0 - C)]$ versus t.

The models described in sections 4.2.4 were fitted to experimental breakthrough curves using linear or non-linear regression methods. Coefficients of linearity (R^2) describe the fit between experimental data and linearized forms of BDST, non-linearized forms of Thomas, Clark, and Yoon-Nelson equations, whereas the sum of the squares of the errors (SSE) calculated according to Eq. (9) indicates the fit between the experimental and predicted values of C/Co used for plotting the breakthrough curves.

$$SSE = \sum_{i=1}^{n} (y_c - y_e)^2 \ , \quad (9)$$

where the subscripts ‘c’ and ‘e’ show the calculated and experimental values, respectively, and n is the number of measurements.

4.3 Results and discussion

4.3.1 Characterization of Mg_3-Fe LDH adsorbent

Fig. 4-1 shows the XRD patterns of raw Mg_3-Fe LDH, calcined Mg_3-Fe LDH, and calcined Mg_3-Fe LDH after adsorption. The diffract grams have typical peaks at d_{003}, d_{006}, d_{012}, d_{110}, and d_{113}, indicating the existence of the Mg-Fe LDH structure. The basal spacing of each labeled sample in Fig. 3-1 is similar to those reported in other studies (Reichle, 1986, Fernández et al, 1998, Kovanda et al, 2003). The raw Mg-Fe LDH was found to have the highest degree of crystallinity by observing the intensity of the characteristic reflection peaks, and after calcination, the crystallinity was lowered as indicated by the broadening and attenuation of the peaks. This occurs because calcination removes the interlayer water and anions, resulting in a partially mixed metal oxide. After being exposed to the phosphate solution, the water is absorbed to re-form the hydroxyl layers, and the phosphate ions and water are incorporated into the interlayer galleries, contributing to the restoration of the typical LDH peaks. The conversion of the mixed metal oxides into LDHs in an aqueous environment is known as the "memory effect," in which the adsorption capacity of the calcined LDHs is greater than that of their precursors. The SEM images show that each sample has a hexagonal plate-like structure that is typical characteristic of LDH materials.

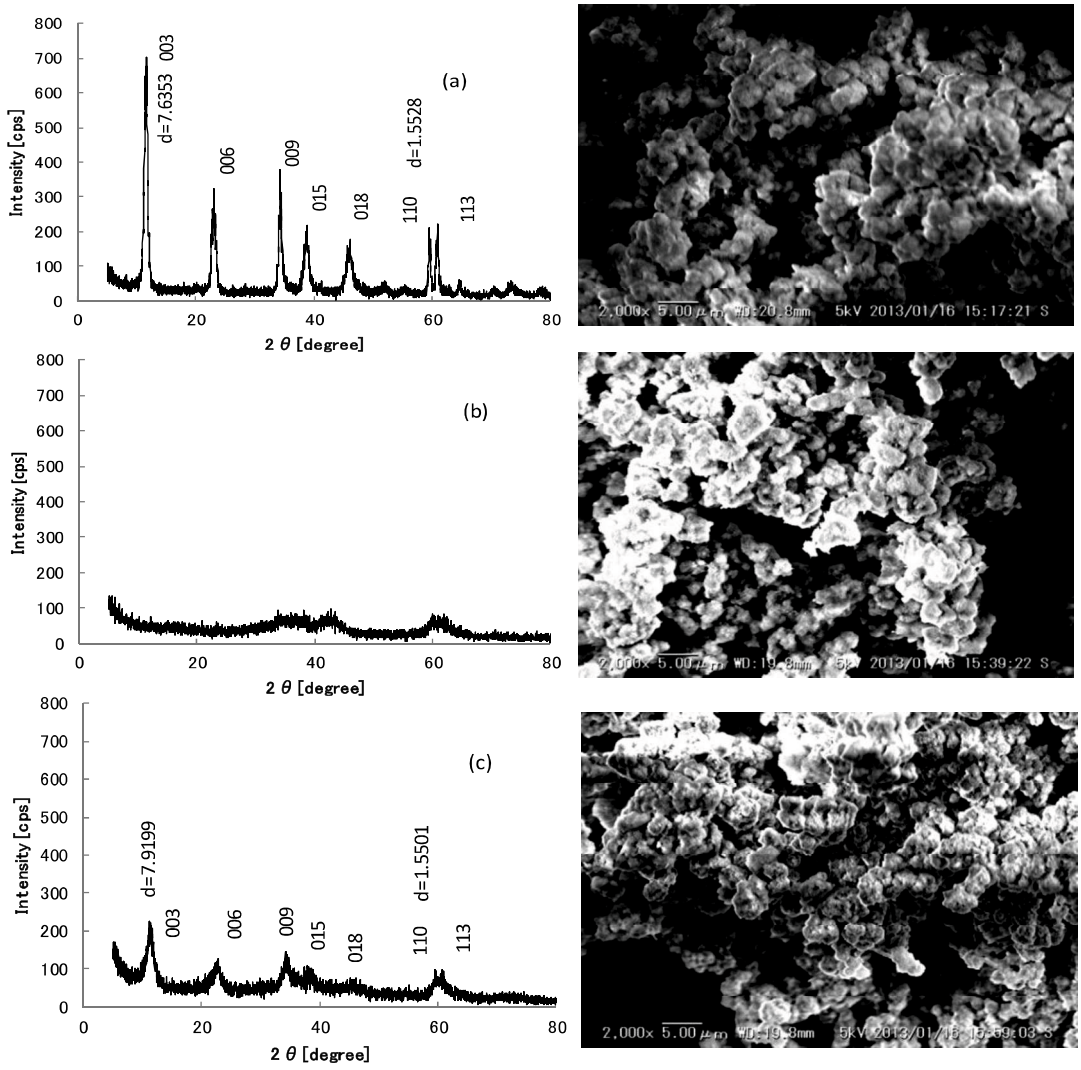

Fig. 4-1 XRD patterns and SEM images of (a) raw Mg_3-Fe LDH, (b) calcined Mg_3-Fe LDH, and (c) calcined Mg-Fe LDH after adsorption.

4.3.2 Effect of bed height on breakthrough curves

Fig. 4-2 presents the performance of breakthrough curves with various bed heights (Z) at a constant flow rate (Q) of 0.024 L/h using a 10 mg/L initial phosphate concentration (C_0) (NaH_2PO_4 solution). It was observed that both the breakthrough and exhaustion times were extended with increasing bed heights (from 6 to 12 to 18 cm), which might be due to the longer bed height allowing a longer empty bed contact time (EBCT) between the adsorbent and adsorbate. Furthermore, the slope of the breakthrough curve became flatter with increasing bed heights, which resulted in a broadened mass transfer zone; the column seemingly took a much longer time to

reach complete exhaustion. Similarly, the equilibrium adsorption capacities (q_e) were found to be 11.58, 13.58, and 14.92 mg-P/g when the bed heights were 6, 12, and 18 cm, respectively (Table 4-1). This increasing tendency could be attributed to a more adsorbent surface area, which provided more binding sites for phosphate adsorption (Nur et al).

Table 4-1 Adsorption breakthrough data for different bed heights, flow rates, and initial phosphate concentrations.

Z **(cm)**	***Q*** **(L/h)**	C_0 **(mg/L)**	t_b **(h)**	V_b **(L)**	**EBCT (h)**	q_e **(mg-P/g)**
6	0.024	10	1.91	0.0455	0.0389	11.58±0.13
12	0.024	10	5.44	0.1332	0.0755	13.58±0.13
18	0.024	10	10.41	0.2499	0.1154	14.92±0.07
12	0.012	10	15.20	0.1974	0.1422	14.91±0.06
12	0.024	10	5.44	0.1332	0.0755	13.58±0.13
12	0.036	10	2.90	0.1060	0.0505	12.20±0.11
12	0.024	5	10.26	0.2432	0.0779	12.28±1.47
12	0.024	10	5.44	0.1332	0.0755	13.58±0.13
12	0.024	20	4.07	0.0966	0.0778	21.09±0.49

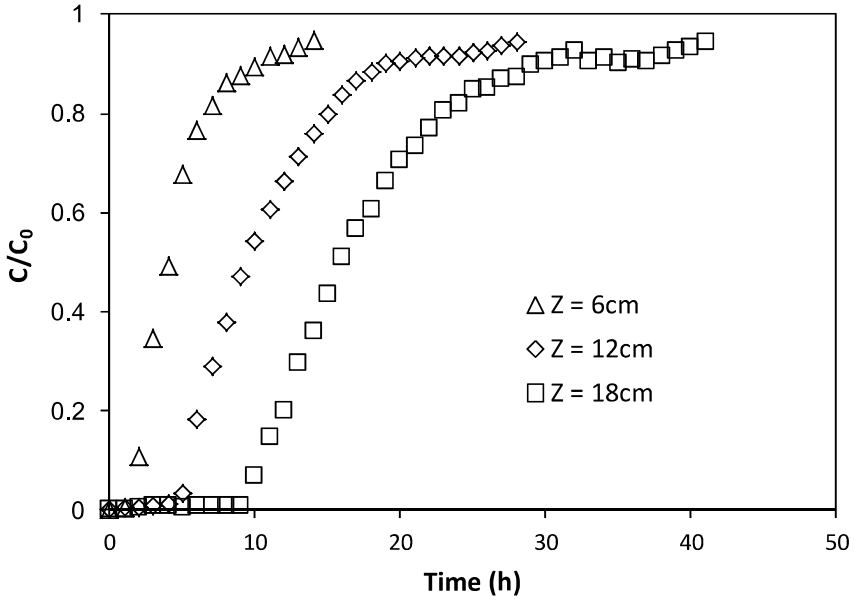

Fig. 4-2 Effect of bed height on the breakthrough curve (C_0 = 10 mg/L, Q = 0.024 L/h).

4.3.3 Effect of flow rate on breakthrough curves

Fig. 4-3 shows the breakthrough curve performance for a bed height of 12 cm and initial phosphate concentration of 10 mg/L. The flow rate varied between 0.012 and 0.036 L/h in the range of 1.5 to 7.5 min, which is within the typical EBCT range, after conversion to EBCT. The figure illustrates that higher flow rates resulted in lowered breakthrough times and volumes because the increasing flow rate corresponded to a decrease in the EBCT. The flow rate also influenced the adsorption capacity, because when the flow rate was increased from 0.012 to 0.036 L/h, the adsorption capacity slightly decreased from 14.91 to 12.20 mg-P/g; therefore, the lower flow rate provided for more efficient interaction between the adsorbent and adsorbate in the solution. Similar phenomena have been observed by other researchers (Bhakat et al, 2007, Unuabonah et al, 2012).

.

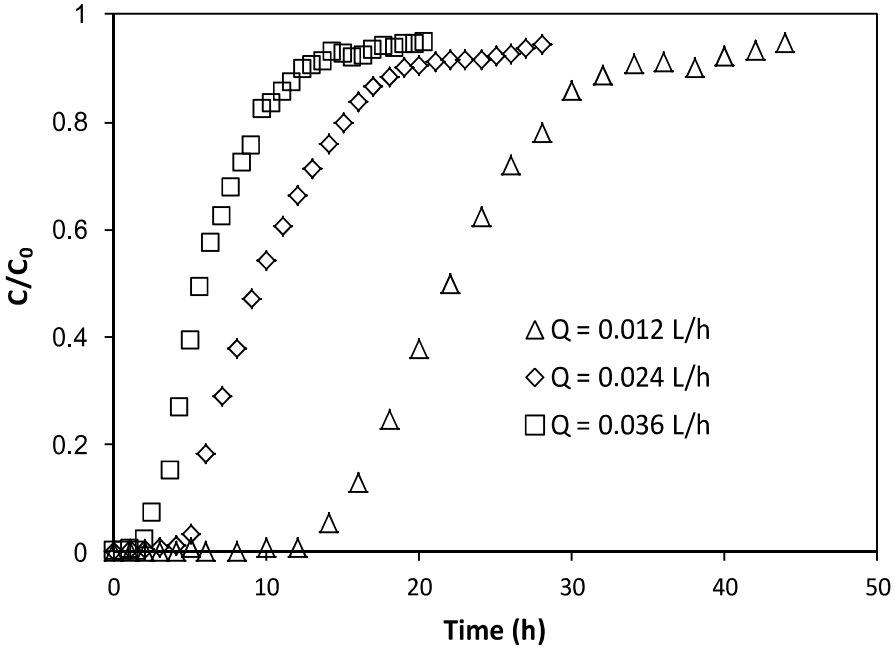

Fig. 4-3 Effect of flow rate on the breakthrough curve (C_0 = 10 mg/L, Z = 12 cm).

4.3.4 Effect of initial phosphate concentration on breakthrough curves

In order to investigate the effect of the initial phosphate concentration on the profiles of the breakthrough curves, a variety of initial concentrations (5, 10, and 20 mg/L) were used under a constant flow rate and with a fixed bed height. As shown in Fig. 4-4, increasing the initial concentration resulted in an earlier breakthrough curve, and the lowest initial concentration treated the highest volume because of the increased diffusion coefficient or mass transfer coefficient. Along our expectations, the phosphate uptake capacities were found to be 12.28, 13.58, and 21.09 mg-P/g when the initial concentrations were 5, 10, and 20 mg/L, respectively. This increase in capacity could be explained by the fact that a higher influent phosphate concentration provided a higher driving force for the transfer process to overcome the mass transfer resistance (Chen et al, 2012). The adsorbent solid/influent liquid (S/L) ratio would be 0.4 if the treated influent volume was assumed to be 0.5 L, and it could be found that the adsorption capacity was 34.5 mg-P/g in a batch test under the same S/L ratio when the initial phosphate concentration was 20 mg/L. The corresponding capacity was 21.09 mg-P/g, which is lower than the previously mentioned capacity because of the insufficient contact time between the adsorbate and the adsorbent in column tests as opposed to batch tests (Srivastava et al, 2008).

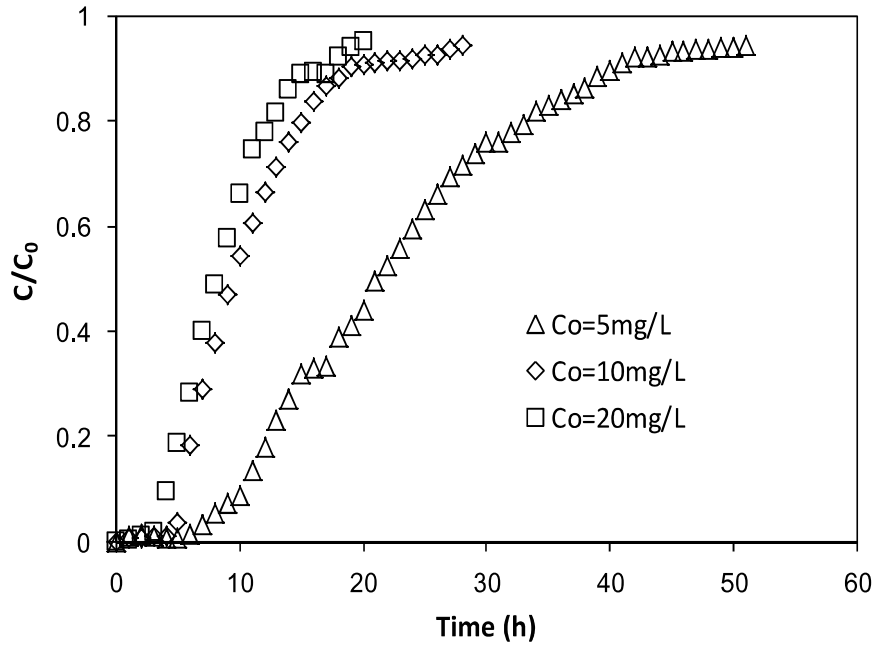

Fig. 4-4 Effect of initial phosphate concentration on the breakthrough curves (Q = 0.024 L/h, Z = 12cm).

4.3.5 Breakthrough curve modeling

Analysis using the BDST model

The BDST plots for phosphate removal at 10%, 20%, 40%, and 60% breakthroughs for a flow rate of 0.024 L/h and an initial concentration of 10 mg/L are shown in Fig. 4-5. The k, N_0, and R^2 values were calculated from the slope and intercept of these plots. From Table 4-2, it can be seen that there was a consistent rise in the slopes from the breakthroughs of 10–60% and a subsequent increase in the corresponding adsorption capacity from 1104.95 to 1742.05 mg-P^-/g. At a lower breakthrough value, some active sites of the adsorbent were still not occupied by phosphate anions; thus, it remained unsaturated. The adsorption capacity at such a low breakthrough condition was therefore bound to be lower than the total fixed-bed capacity of the adsorbent. Another noteworthy finding from Fig. 4-5 was that the extrapolated linear regression of the 50% breakthrough did not pass through the origin. Theoretically, C/C_0 is 0.5 at 50% breakthrough; therefore, the logarithmic term of Eq. (3) becomes 0, and the 50% breakthrough should be a straight line passing through the origin at t = 0 h. This

nonconformity indicates that the transport of phosphate from the aqueous solution onto the calcined Mg_3-Fe LDH adsorbent involves more than one rate-limiting step (Sharma and Forster, 1995). The values of R^2 were above 0.99, indicating the validity of the BDST model for the column system at breakthroughs below 60%. Additionally, the obtained BDST model constants can be useful for the theoretical predictions of scaling up the process for other flow rates and initial concentration conditions (Kumar and Chakraborty, 2009).

Table 4-2 Parameters of BDST model using linear regression analysis (C_0 = 10 mg/L, Q = 0.024 L/h).

C/C_0	a (h/cm)	b (h)	$k_a \times 10^2$ (L/mg h)	N_0 (mg/L)	R^2	SSE
0.1	0.7083	-2.5000	8.79	1104.95	0.9897	0.38
0.2	0.8000	-2.6333	5.26	1248.00	0.9930	0.33
0.4	0.9000	-1.9000	2.13	1404.00	0.9959	0.24
0.6	1.1167	-2.1333	-1.90	1742.05	0.9988	0.11

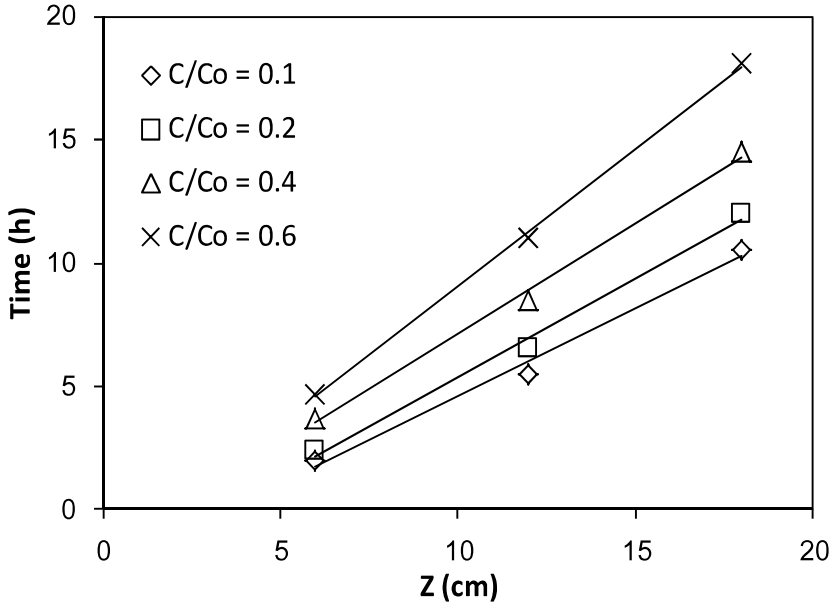

Fig. 4-5 Times of breakthroughs with respect to bed height according to the BDST model. (Q = 0.024 L/h, C_0 = 10 mg/L).

Analysis using the Thomas model

The Thomas model was applied to the experimental data for C/C_0 ratios ranging from 0.08 to 0.95 while varying bed height, flow rate, and initial phosphate concentration. As listed in Table 4-3, when Z was increased, the value of k_T decreased, and the value of Q_0 increased. As Q increased, the value of k_T increased, and the value of q_0 decreased from 14.36 mg-P/g to 12.06 mg-P/g, implying that in the range of 0.12 to 0.36 L/h, the fluctuations in flow rate has slight effect on the adsorption efficiency. When C_0 increased, the value of q_0 noticeably increased, but the value of k_T decreased. This is attributed to the difference in driving force for adsorption that accompanies the concentration difference. Therefore, the higher driving force resulting from higher phosphate ion concentration led to a higher q_0 value (Chen,Yue, 2012). Additionally, it was found that the values of q_0 estimated using the Thomas model are very close to the q_e values calculated from experimental results with varying Q, Z and C_0 conditions. The high values of non-linear regression coefficients demonstrated the adequacy of the linearized Thomas model equation to fit the experimental data along a non-linear regression (Table 4-3). Furthermore, comparing the R^2 and SSE values for various models revealed that the Thomas model suitably described the LDH adsorption process in a fixed-bed column where the diffusion through the film/pores is not the rate limiting step.

Table 4-3 Parameters of the Thomas model using linear regression analysis at various bed heights, flow rates, and initial phosphate concentrations.

Z (cm)	*Q (L/h)*	*C_0 (mg/L)*	*k_T ×10^2L/(mg h)*	*q_0 (mg-P/g)*	*R^2*	*SSE*
6	0.024	10	6.57	10.28	0.9624	0.061
12	0.024	10	3.27	12.25	0.9735	0.096
18	0.024	10	2.44	13.84	0.9772	0.133
12	0.012	10	2.55	14.36	0.9914	0.034
12	0.024	10	3.27	12.25	0.9735	0.096
12	0.036	10	4.77	12.06	0.9750	0.098
12	0.024	5	2.95	12.89	0.9873	0.078
12	0.024	10	3.27	12.25	0.9735	0.096
12	0.024	20	1.96	20.46	0.9834	0.078

Analysis using the Clark model

The value of the Freundlich constant (n = 1.4), which was obtained from the batch tests in our previous work, was used in the Clark model to calculate the other model parameters, A and r, which were, respectively, determined from Eq. (5). The observed increase in the rate of mass transfer (r) with increasing flow rate was because the higher flow rates shorten the distance for the molecular diffusion of adsorbates through the stationary layer of water that surrounds adsorbent particles. The rate of mass transfer also increased with increasing initial phosphate concentration and with it, the driving force and mass transfer of the adsorbate to the adsorbent surface. However, a greater bed height can be attributed to an increased adsorbent dosage; thus, there is an increased number of particles available for interaction, thus reducing the mass transfer rate (Aksu and Gönen, 2004).

As seen in Table 4-4, R^2 values were high (ranging from 0.9747 to 0.9955) and the corresponding SSE values were lower, indicating that the Clark model best predicts the breakthrough curve of LDH adsorption process among all tested models, meanwhile, the behavior of this system was simulated as a Freundlich adsorption,

which matched our conclusion from previous batch study .

Table 4-4 Parameters of the Clark model using linear regression analysis at various bed heights, flow rates, and initial phosphate concentrations.

Z (cm)	*Q (L/h)*	*C_0 (mg/L)*	*r ×10(1/h)*	*A*	*R^2*	*SSE*
6	0.024	10	5.25	2.93	0.9747	0.041
12	0.024	10	2.63	4.48	0.9834	0.060
18	0.024	10	1.99	8.93	0.9855	0.085
12	0.012	10	1.99	26.84	0.9955	0.018
12	0.024	10	2.63	4.48	0.9834	0.060
12	0.036	10	3.91	3.67	0.9845	0.061
12	0.024	5	1.16	3.96	0.9947	0.033
12	0.024	10	2.63	4.48	0.9834	0.060
12	0.024	20	3.15	4.49	0.9922	0.020

Analysis using the Yoon-Nelson model

A simple theoretical model was introduced to investigate the breakthrough behavior of phosphate adsorption on Mg_3Fe LDH adsorbent. The values of k_Y, $t_{0.5}$, and other statistical parameters are listed in Table 4-5. As shown in Table 4-5, the value of k_Y was found to decrease with increasing bed height, but it decreases proportionally with flow rate and initial concentration, whereas the t value showed an opposite trend. The values of $t_{0.5}$ were found to be much lower than the experimental t value at 50% breakthrough under all conditions, indicating that the Yoon-Nelson model is not very accurate in predicting the $t_{0.5}$ value because of its relative simplicity.

Table 4-5 Parameters of the Yoon-Nelson model using linear regression analysis at various bed heights, flow rates, and initial phosphate concentrations.

Z (cm)	*Q (L/h)*	*C_0 (mg/L)*	*$t_{0.5}$(h)*	*k_Y ×10 (1/h)*	*R^2*	*SSE*
6	0.024	10	0.48	2.15	0.9720	0.12

12	0.024	10	1.90	1.10	0.9383	0.48
18	0.024	10	5.89	0.80	0.9121	0.88
12	0.012	10	13.85	0.97	0.9566	0.30
12	0.024	10	1.90	1.10	0.9383	0.48
12	0.036	10	-1.56	1.39	0.9237	0.92
12	0.024	5	14.72	0.82	0.9679	0.47
12	0.024	10	1.90	1.10	0.9383	0.48
12	0.024	20	6.88	2.29	0.9834	0.11

4.3.6 Mechanism studies

Mechanism studies are important in understanding the interaction between adsorbent and adsorbate, which leads to optimize the operation parameters for adsorption and desorption process. The XRD patterns of the LDH before and after adsorption have been shown in Fig. 3-1. The forms of LDH sample still showed typical peak of crystallinity after adsorption of phosphate, which suggested a preservation of the structure. According to a 3R polytypism, the refined cell parameter a (a=2d(110)) is the metal-metal distance in the layer, c(c=3d(003)) is the interlayer distance. The LDH with different interlayer anion can be identified by observing interlayer distance. It was found that a value nearly did not change, however c value changed significantly from 22.91Å to 23.76 Å after phosphate adsorption, which means the interlayer anion was replaced by phosphate anion. This phenomenon might be proved that ion exchange is the main mechanism for the adsorption process. As we concluded that Clark model had best fitness with experimental data in previous discussion, it could be deduced that the adsorption isotherm obeyed Freundlich model, indicating there is a multilayer reaction during adsorption process, meanwhile the mass transfer process was considered as an unneglectable factor since it limited the reaction rate, especially in a fix-bed column system. A hypothetical mechanism could be followed three steps: (1) external mass transfer such as adsorbate being transported

from bulk solution to the boundary layer of water surrounding the adsorbent particle. (2) intra-particle transports such adsorbate being transported through the adsorbent's pores to available adsorption site. (3) Adsorption reaction dominated by ion exchange process substituted of interlayer anion by phosphate anion.

4.3.7 Phosphate adsorption from anaerobic sludge filtrate

Adsorption breakthrough curve

The anaerobic sludge sample was obtained from the eastern municipal wastewater treatment plant in Ube, Japan. After 24 h of sedimentation, the supernatant was filtered through a 0.45 μm membrane and this filtrate was used for the subsequent column tests. The pH and anion components are listed in Table 4-6. A multicomponent adsorption breakthrough curve using a filtered matrix of anaerobic sludge is compared to a phosphate adsorption breakthrough curve (using pure NaH_2PO_4 solutions) in Fig. 4-6. The profile of breakthrough curves of Cl^- and NO_3^- approximate to horizontal lines, indicating that almost no adsorption of these anions occurs through the column until it reaches the outlet. The breakthrough of SO_4^{2-} started quite early; the breakthrough then proceeded rapidly until SO_4^{2-} was exhausted at 6 h, indicating that the SO_4^{2-} anion is a significantly less-preferred adsorbate on LDH adsorbent as compared to PO_4^{3-}, and only a tiny amount of SO_4^{2-} is adsorbed during the entire run. All of these observations were found to be consistent with the results of phosphate adsorption selectivity during the batch tests of our previous research and of other studies (Das,Patra, 2006, He et al, 2010). The breakthrough of PO_4^{3-} occurred at approximately 3 h and tended to exhaust more gradually until complete exhaustion at approximately 72 h. The breakthrough point occurred earlier than we expected based on the assumption that the pure NaH_2PO_4 solution had the same phosphate concentration as in the actual anaerobic sludge filtrate, in which case the breakthrough time should be between 5.44 h (10 mg/L initial concentration) and 4.07 h (20 mg/L initial concentration) as listed in Table 4-1. The premature breakthrough is probably due to impurities, especially tiny suspended

solids in the sludge filtrate that interfere with the mass transfer between liquid and solid phases (Cheng,Huang, 2010).

Table 4-6 Characteristics of anaerobic sludge filtrate.

Parameter	***Value***
pH	6.80
SS (mg/L)	3.82
COD (mg/L)	404.52
NO_2^- (mg/L)	1.68
NO_3^- (mg/L)	18.00
Cl^- (mg/L)	62.20
SO_4^{2-} (mg/L)	149.38
PO_4^{3-} (mg/L)	12.29

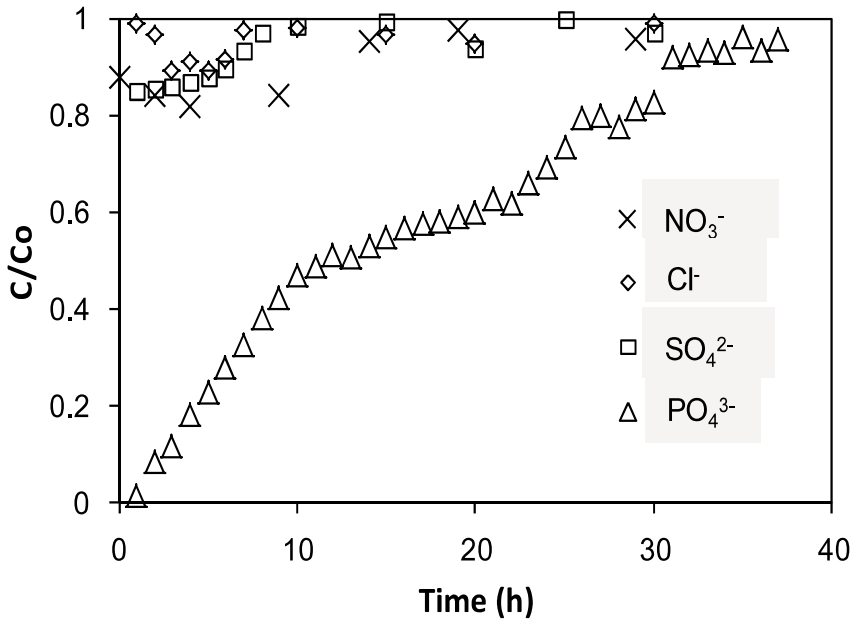

Fig. 4-6 Breakthrough curves of various anions in anaerobic sludge filtrate (NO_2^-could not be detected).

Phosphate adsorption/desorption and reusability

Because reversible ion-exchange reactions are the most useful type, the exhausted

bed is regenerated using an excess of presaturated ions. Recently, various alkaline solutions, salt solutions, and mixtures thereof have been used to achieve satisfactory desorption from calcined Mg_3-Fe LDH (Kuzawa et al, 2006, Cheng,Huang, 2009, Chitrakar et al, 2010). In our previous study, a 1 M NaOH desorption solution was found to reach the highest desorption efficiency (76.4%), whereas a 0.1 M NaOH solution exhibited a very close desorption efficiency (73.4%). From an economic standpoint, a 0.1 M NaOH solution was used in this series of column tests. Fig. 4-7 shows the results of the adsorption and desorption cycles, which were repeated up to 5 times. The phosphate uptake in the first cycle was 24.64 mg-PO_4^{3-}/g, and it gradually decreased to 13.52 mg-PO_4^{3-}/g after 5 cycles, which is approximately 55% of initial phosphate adsorption capacity. The results indicate that increasing the number of adsorption cycles increase the destruction of the layered structure, leading to the capacity loss. On the other hand, the desorption rate was maintained at approximately 50% even after 5 cycles, indicating that the adsorbent may be suitable for practical applications. I presume the reason for the insufficient desorption rate is the assumption that the initial adsorbed phosphate ions were bound through strong interactions within the layer or replaced by irreversible fouling in the LDHs (Anirudhan et al, 2006).

Although it was confirmed that the adsorbent could still exhibit satisfactory phosphate adsorption capacity in an anaerobic sludge filtrate consisting of SO_4^{2-}, NO_3^-, and Cl^- in addition to PO_4^{3-}, several important considerations should be taken in the design of LDH adsorption systems. 1) The supernatant from the anaerobic sludge filtrate contains medium suspended solids, which could foul the ion exchanger and cause potential clogging problems. Therefore, an economical pretreatment such as dual-media or multi-media filters would be required for a pilot application. 2) The further processing of recovered phosphate from phosphate-desorbed alkaline solution to useful finalized products such as calcium phosphate, hydroxyapatite, or magnesium ammonium phosphate need to be investigated, and the proper disposal of the restored desorption solution also needs to be addressed.

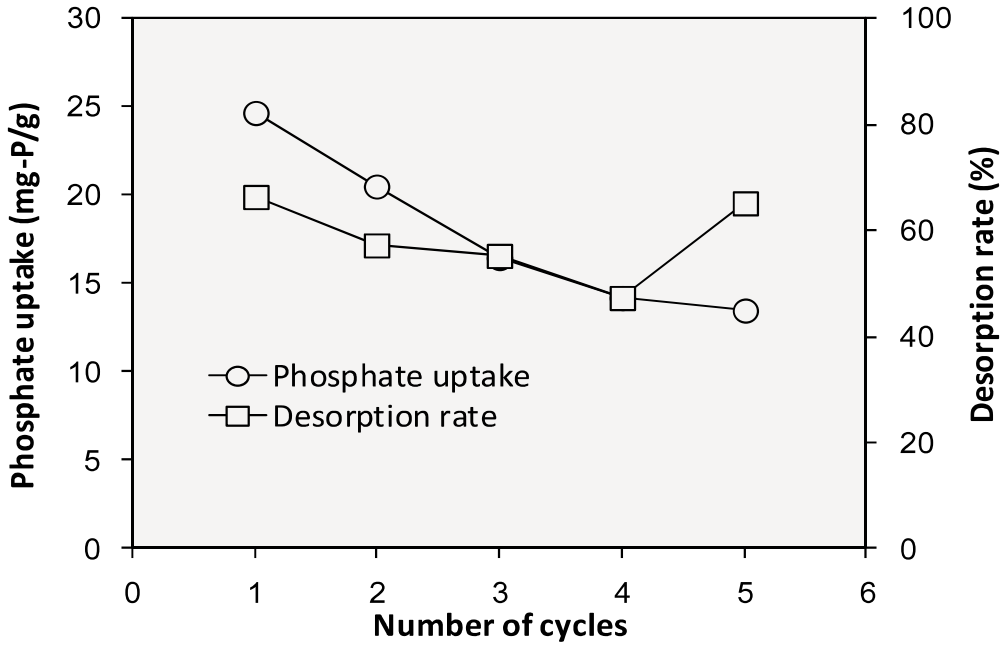

Fig. 4-7 Phosphate uptake and reusability in cycle assays.

4.4 Conclusions

In this study, the phosphate adsorption performance of calcined Mg_3-Fe LDH adsorbent was investigated in a continuous fixed-bed column. The effects of bed height, flow rate, and initial phosphate concentration on the adsorption capacity and breakthrough curve profiles were investigated. It was found that an increase in bed height and initial phosphate concentration or a decrease of flow rate improves the adsorption capacity. The BDST model was found to satisfactorily predict the breakthrough curve up to 60% breakthrough at a 0.024 L/h flow rate and 10 mg/L initial phosphate concentration. The Clark model was found to be the most suitable for fitting experimental data with respect to various bed heights, flow rates, and initial phosphate concentration values, followed by the Thomas and Yoon-Nelson models (in decreasing order of suitability). It was found that applicability of this adsorbent to phosphate recovery from anaerobic sludge filtrate because of its good selectivity in a system of coexisting anions, high adsorption capacity, and acceptable reusability.

4.5 Reference

Aksu, Z. and F. Gönen. 2004. Biosorption of phenol by immobilized activated sludge in a continuous packed bed: prediction of breakthrough curves. *Process Biochemistry*, **39**(5), 599-613.

Álvarez-Ayuso, E. and H.W. Nugteren. 2005. Purification of chromium(VI) finishing wastewaters using calcined and uncalcined Mg-Al-CO3-hydrotalcite. *Water Research*, **39**(12), 2535-2542.

Anirudhan, T.S., B.F. Noeline, and D.M. Manohar. 2006. Phosphate Removal from Wastewaters Using a Weak Anion Exchanger Prepared from a Lignocellulosic Residue. *Environmental Science & Technology*, **40**(8), 2740-2745.

Bhakat, P.B., A.K. Gupta, and S. Ayoob. 2007. Feasibility analysis of As(III) removal in a continuous flow fixed bed system by modified calcined bauxite (MCB). *Journal of Hazardous Materials*, **139**(2), 286-292.

Carja, G., R. Nakamura, and H. Niiyama. 2005. Tailoring the porous properties of iron containing mixed oxides for As (V) removal from aqueous solutions. *Microporous and Mesoporous Materials*, **83**(1-3), 94-100.

Chen, S., Q. Yue, B. Gao, Q. Li, X. Xu, and K. Fu. 2012. Adsorption of hexavalent chromium from aqueous solution by modified corn stalk: A fixed-bed column study. *Bioresource Technology*, **113**(0), 114-120.

Cheng, X., X. Huang, X. Wang, and D. Sun. 2010. Influence of calcination on the adsorptive removal of phosphate by Zn-Al layered double hydroxides from excess sludge liquor. *Journal of Hazardous Materials*, **177**(1-3), 516-523.

Cheng, X., X. Huang, X. Wang, B. Zhao, A. Chen, and D. Sun. 2009. Phosphate adsorption from sewage sludge filtrate using zinc–aluminum layered double hydroxides. *Journal of Hazardous Materials*, **169**(1-3), 958-964.

Chibwe, K. and W. Jones. 1989. Intercalation of organic and inorganic anions into layered double hydroxides. *Journal of the Chemical Society, Chemical Communications*, 14), 926-927.

Chitrakar, R., S. Tezuka, J. Hosokawa, Y. Makita, A. Sonoda, K. Ooi, and T. Hirotsu. 2010. Uptake properties of phosphate on a novel Zr-modified MgFe-LDH(CO3). *Journal of Colloid and Interface Science*, **349**(1), 314-320.

Chitrakar, R., S. Tezuka, A. Sonoda, K. Sakane, K. Ooi, and T. Hirotsu. 2005. Adsorption of phosphate from seawater on calcined MgMn-layered double hydroxides. *Journal of Colloid and Interface Science*, **290**(1), 45-51.

Clark, R.M. 1987. Evaluating the cost and performance of field-scale granular activated carbon systems. *Environmental Science & Technology*, **21**(6), 573-580.

Cordell, D., J.-O. Drangert, and S. White. 2009. The story of phosphorus: Global food security and food for thought. *Global Environmental Change*, **19**(2), 292-305.

Das, J., B.S. Patra, N. Baliarsingh, and K.M. Parida. 2006. Adsorption of phosphate by layered double hydroxides in aqueous solutions. *Applied Clay Science*, **32**(3-4), 252-260.

de-Bashan, L.E. and Y. Bashan. 2004. Recent advances in removing phosphorus from wastewater and its future use as fertilizer (1997–2003). *Water Research*, **38**(19), 4222-4246.

Fernández, J.M., M.A. Ulibarri, F.M. Labajos, and V. Rives. 1998. The effect of iron on the crystalline phases formed upon thermal decomposition of Mg-Al-Fe hydrotalcites. *Journal of Materials Chemistry*, **8**(11), 2507-2514.

He, H., H. Kang, S. Ma, Y. Bai, and X. Yang. 2010. High adsorption selectivity of ZnAl layered double hydroxides and the calcined materials toward phosphate. *Journal of Colloid and Interface Science*, **343**(1), 225-231.

Hutchins, R.A. 1973. New method simplifies design of activated-carbon system. *Chemical Engineering*, **80**(133-138.

Kameda, T., T. Yoshioka, M. Uchida, and A. Okuwaki. 2002. Synthesis of hydrotalcite from seawater and its application to phosphorus removal. *Phosphorus, Sulfur and Silicon and Related Elements*, **177**(6-7), 1503-1506.

Kovanda, F., V. Balek, V. Dorničák, P. Martinec, M. Mašláň, L. Bílková, D. Koloušek, and I.M. Bountsewa. 2003. Thermal behaviour of synthetic pyroaurite-like anionic clay. *Journal of Thermal Analysis and Calorimetry*, **71**(3), 727-737.

Kumar, P.A. and S. Chakraborty. 2009. Fixed-bed column study for hexavalent chromium removal and recovery by short-chain polyaniline synthesized on jute fiber. *Journal of Hazardous Materials*, **162**(2–3), 1086-1098.

Kuzawa, K., Y.-J. Jung, Y. Kiso, T. Yamada, M. Nagai, and T.-G. Lee. 2006. Phosphate removal and recovery with a synthetic hydrotalcite as an adsorbent. *Chemosphere*, **62**(1), 45-52.

Lazaridis, N.K., A. Hourzemanoglou, and K.A. Matis. 2002. Flotation of metal-loaded clay anion exchangers. Part II: the case of arsenates. *Chemosphere*, **47**(3), 319-324.

Li, F. and X. Duan. 2006 *Applications of Layered Double Hydroxides, Layered Double Hydroxides*. Springer Heidelberg.

Mino, T., M.C.M. van Loosdrecht, and J.J. Heijnen. 1998. Microbiology and biochemistry of the enhanced biological phosphate removal process. *Water Research*, **32**(11), 3193-3207.

Nur, T., M.A.H. Johir, P. Loganathan, T. Nguyen, S. Vigneswaran, and J. Kandasamy. Phosphate removal from water using an iron oxide impregnated strong base anion exchange resin. *Journal of Industrial and Engineering Chemistry*, 0),

Reichle, W.T. 1986. Synthesis of anionic clay minerals (mixed metal hydroxides, hydrotalcite). *Solid State Ionics*, **22**(1), 135-141.

Richard, S. 1991 *Phosphorus and Nitrogen Removal from Municipal Wastewater*. Lewis Publishers, New York.

Sharma, D.C. and C.F. Forster. 1995. Column studies into the adsorption of chromium (VI) using sphagnum moss peat. *Bioresource Technology*, **52**(3), 261-267.

Song, Y., P. Yuan, B. Zheng, J. Peng, F. Yuan, and Y. Gao. 2007. Nutrients removal and recovery by crystallization of magnesium ammonium phosphate from synthetic swine wastewater. *Chemosphere*, **69**(2), 319-324.

Srivastava, V.C., B. Prasad, I.M. Mishra, I.D. Mall, and M.M. Swamy. 2008. Prediction of Breakthrough Curves for Sorptive Removal of Phenol by Bagasse Fly Ash Packed Bed. *Industrial & Engineering Chemistry Research*, **47**(5), 1603-1613.

Sun, X., T. Imai, M. Sekine, T. Higuchi, K. Yamamoto, and K. Akagi. 2013. Adsorption of Phosphate by Calcinated Mg-Fe Layered Double Hydroxide. *Journal of Water and Environment Technology*, **11**(2), 111-120.

Thomas, H.C. 1944. Heterogeneous Ion Exchange in a Flowing System. *Journal of the American Chemical Society*, **66**(10), 1664-1666.

Unuabonah, E.I., M.I. El-Khaiary, B.I. Olu-Owolabi, and K.O. Adebowale. 2012. Predicting the dynamics and performance of a polymer–clay based composite in a fixed bed system for the removal of

lead (II) ion. *Chemical Engineering Research and Design*, **90**(8), 1105-1115.

Yang, L., Z. Shahrivari, P.K.T. Liu, M. Sahimi, and T.T. Tsotsis. 2005. Removal of trace levels of arsenic and selenium from aqueous solutions by calcined and uncalcined layered double hydroxides (LDH). *Industrial and Engineering Chemistry Research*, **44**(17), 6804-6815.

Yoon, Y.H. and J.H. Nelson. 1984. Application of Gas Adsorption Kinetics I. A Theoretical Model for Respirator Cartridge Service Life. *American Industrial Hygiene Association Journal*, **45**(8), 509-516.

CHAPTER 5

CONCLUSION AND FUTURE WORK

A novel calcined Mg_3-Fe LDH was synthesized to investigate the phosphate adsorption performance. A high phosphate adsorption capacity, good adsorption selectivity and satisfactory desorption efficiency were found on batch experiments as well as the adsorption dynamic kinetics were approved to follow pseudo-second-order model and adsorption isotherms to follow Freundlich model. The breakthrough curves were used to describe the adsorption process of phosphate on this adsorbent on continuous experiments and were found that an increase in bed height and initial phosphate concentration or a decrease of flow rate improves the adsorption capacity. Furthermore, several models were introduced to fit the adsorption breakthrough curves, the results indicated that the BDST model was found to satisfactorily predict the breakthrough curve up to 60% breakthrough at a 0.024 L/h flow rate and 10 mg/L initial phosphate concentration, the Clark model was found to be the most suitable for fitting experimental data with respect to various bed heights, flow rates, and initial phosphate concentration values, followed by the Thomas and Yoon-Nelson models (in decreasing order of suitability). Finally, the adsorbent was applied to actual anaerobic sludge filtrate and proved to have good selectivity in a system of coexisting anions, high adsorption capacity, and acceptable reusability.

Although it was confirmed that the adsorbent could still exhibit satisfactory phosphate adsorption capacity in an anaerobic sludge filtrate consisting of SO_4^{2-}, NO_3^-, and Cl^- in addition to PO_4^{3-}, several important considerations should be taken in the design of LDH adsorption systems. 1) The supernatant from the anaerobic sludge filtrate contains medium suspended solids, which could foul the ion exchanger and cause potential clogging problems. Therefore, an economical pretreatment such as dual-media or multi-media filters would be required for a pilot application. 2) The further processing of recovered phosphate from phosphate-desorbed alkaline solution

to useful finalized products such as calcium phosphate, hydroxyapatite, or magnesium ammonium phosphate need to be investigated, and the proper disposal of the restored desorption solution also needs to be addressed.

PUBLICATION LIST

1. **XiaoFeng SUN**, Tsuyoshi IMAI, Masahiko SEKINE, Takaya HIGUCHI, Koichi, YAMAMOTO, Kenji AKAGI. (**2013**) Adsorption of phosphate by calcinated Mg-Fe layered double hydroxide. Journal of Water and Environment Technology.11 (2): 111-120.

2. **XiaoFeng SUN**, Tsuyoshi IMAI, Masahiko SEKINE, Takaya HIGUCHI, Koichi, YAMAMOTO, Ariyo KANNO. (**2013**) Adsorption of phosphate using calcined Mg3-Fe layered double hydroxides in a fixed-bed column study. Journal of Industrial and Engineering Chemistry
   (Accepted, 2013.12.19)

PRESENTATIONS

1. **XiaoFeng SUN**, Tsuyoshi IMAI, Masahiko SEKINE, Takaya HIGUCHI, Koichi, YAMAMOTO, Kenji AKAGI. Adsorption of phosphate by calcinated Mg-Fe layered double hydroxide. Water and Environment Technology Conference 2012, Tokyo, Japan. P.42 **(ORAL)**